Spring 1981

An Experimental Comparison of Cross Correlator Performances Based Upon Signal-To-Noise Ratios

Sunder G. Gopani
University of Central Florida

AN EXPERIMENTAL COMPARISON OF CROSS CORRELATOR PERFORMANCES BASED UPON SIGNAL-TO-NOISE RATIOS

BY

SUNDER G. GOPANI
B.Sc., Fergusson College, 1978

RESEARCH REPORT

Submitted in partial fulfillment of the requirements
for the degree of Master of Science
in the Graduate Studies Program of the College of Engineering
at the University of Central Florida at Orlando, Florida

Spring Quarter
1981

AN EXPERIMENTAL COMPARISON OF CROSS CORRELATOR PERFORMANCES BASED UPON SIGNAL-TO-NOISE RATIOS

BY

SUNDER G. GOPANI

ABSTRACT

Three commonly employed types of cross correlators were designed using standardized components which closely simulate idealized elements in an effort to experimentally verify the theoretical analysis. These cross correlators are (1) the standard analog cross correlator which consists of bandpass filters, a multiplier and a postmultiplier lowpass filter, (2) the polarity coincidence correlator (PCC) which utilizes a hard clipper in each input channel, and (3) a modified type of PCC which features a hard clipper in only one of the input channels. Two different types of filters viz. (1) the seventh-order Butterworth lowpass filter, and (2) the five-pole Chebyshev lowpass filter with a maximum passband loss of 1 dB were utilized. The output signal-to-noise ratio (SNR) was experimentally computed as a function of input signal-to-noise ratio and compared with theoretical predictions. The performance in terms of output SNRs of the three cross correlators are compared. In all cases, the experimental results were in close agreement with the theoretical models.

Ronald L. Phillips

Dr. Ronald L. Phillips
Director of Research Report

ACKNOWLEDGEMENTS

It is with great pleasure that I take this opportunity to express my deep appreciation to Dr. Ronald L. Phillips, Dr. Larry C. Andrews, Dr. Michael G. Harris and Mr. Madjid Belkerdid for their substantial help, suggestions and guidance. I am especially grateful to Dr. Brian E. Petrasko for his invaluable advice and inspiration. I also express my thanks to Mr. Chetan Gopani for his diligent support and understanding. Last, but not least, my sincere appreciation goes to Ms. Dian Brandstetter for the typing of the research report.

Orlando, Florida
1981

S.G.G.

TABLE OF CONTENTS

I. INTRODUCTION

Correlation techniques have been increasingly adopted in such diverse applications as radio astronomy, telecommunications, linear systems analysis, radar and sonar systems and statistical optics. This paper is concerned with the application of correlation analysis to the detection of sinusoidal signals corrupted by Gaussian noise.

Essentially the correlation between two random variables is the expected value of their product averaged over a long time. If $f_1(t)$ and $f_2(t)$ are the two sample functions of different stationary random processes then the cross-correlation function is defined as

$$R_{12}(\tau) = \lim_{T\to\infty} \frac{1}{2T} \int_{-T}^{T} f_1(t) f_2(t + \tau) dt \tag{1}$$

and the autocorrelation function of the sample function $f_1(t)$ is defined as

$$R_{11}(\tau) = \lim_{T\to\infty} \frac{1}{2T} \int_{-T}^{T} f_1(t) f_1(t + \tau) dt \tag{2}$$

where τ is the delay time. Practically, the two sample functions $f_1(t)$ and $f_2(t + \tau)$ are continuously multiplied and their product fed through a lowpass filter. The filter output is a close approximation of the true mathematical cross-correlation function and the device is called a cross-correlator.

The analyses of three commonly employed types of cross-correlators are discussed. These are (1) the standard analog correlator (System I) which consists of bandpass filters, a multiplier and a postmultiplier lowpass filter, (2) the polarity coincidence correlator (PCC, referred to as System II) which utilizes clippers prior to the multiplier and (3) a modified PCC (System III) which features a clipper in one of the input channels only. Fig. 1 shows the block diagrams of all three systems.

Both System I and System II have been studied extensively over the last twenty years. Although System III has been used for several years in certain radar and sonar detection systems, it is not widely discussed in the literature as are System I and System II. Andrews (1973, 1974 and 1980) has performed analyses on these three cross-correlators obtaining expressions for the output characteristic functions and/or the output probability density functions (pdf). Relying upon mathematical expressions found in the literature for each system, Allgaier (1979) computed the numerical values of the output signal-to-noise ratio (SNR) as a function of the input SNR in each channel; the performances in terms of output SNR of all three systems were compared.

In all cases the inputs are assumed to be $A \cos \omega_o t + n_1(t)$ and $A \cos \omega_o t + n_2(t)$ where $n_1(t)$ and $n_2(t)$ are zero mean Gaussian noises. These noise terms in the two channels are assumed to be statistically independent. The input signal power is the time average of the square of the signal i.e.,

$$\lim_{T\to\infty} \frac{1}{T} \int_0^T A^2 \cos^2 \omega_o t \, dt = \frac{1}{2} A^2 .$$

σ_1^2 and σ_2^2, the variances of the noise terms, are the input noise power for channel 1 and channel 2 respectively. The input SNR is defined as the ratio of the total input signal power divided by the total input noise power. Thus the input SNRs for the two input channels are

$$S_1 = A^2/2\sigma_1^2 \tag{3}$$

and

$$S_2 = A^2/2\sigma_2^2 . \tag{4}$$

The average output signal power is given by

$$S_o = (m_1 - m_1|_{S_1,\ S_2 = 0})^2$$

where m_1 is the first moment and $m_1|_{S_1,\ S_2 = 0}$ is the same moment when input signals are absent. In our case $m_1|_{S_1,\ S_2 = 0}$ is zero. The total output noise power is defined as the variance of the output i.e., $N_o = (m_2 - m_1^2)$

where m_2 is the second moment. The output SNR is then given by

$$\frac{S_o}{N_o} = \frac{m_1^2}{(m_2 - m_1^2)} . \tag{5}$$

Though the three systems have been intensely analyzed, leading to mathematical expressions like output characteristic functions, output pdfs and output SNRs, none show experimental data to support the theoretical analysis. The primary purpose of this research paper was to provide an experimental comparison of the three cross-correlator performances in terms of output SNRs. Specially built

circuits were fabricated using components which closely simulate idealized elements of each system. Fig. 2 shows the simulated cross-correlators used to test agreement with theoretical predictions. The configuration of the simulated cross-correlators in fig. 2 enabled the amplification of the narrowband noise power to a desiring detectable quantity. In experimental set 1, the postmultiplier lowpass filter is a seventh-order Butterworth lowpass filter whereas in set 2 we utilized a five-pole Chebyshev lowpass filter with a maximum loss of 1 dB in the passband. Data was collected by a computer from which the first two statistical moments were computed. Using (3), (4) and (5), the signal-to-noise ratios were calculated and plotted with the theoretical curves for comparison.

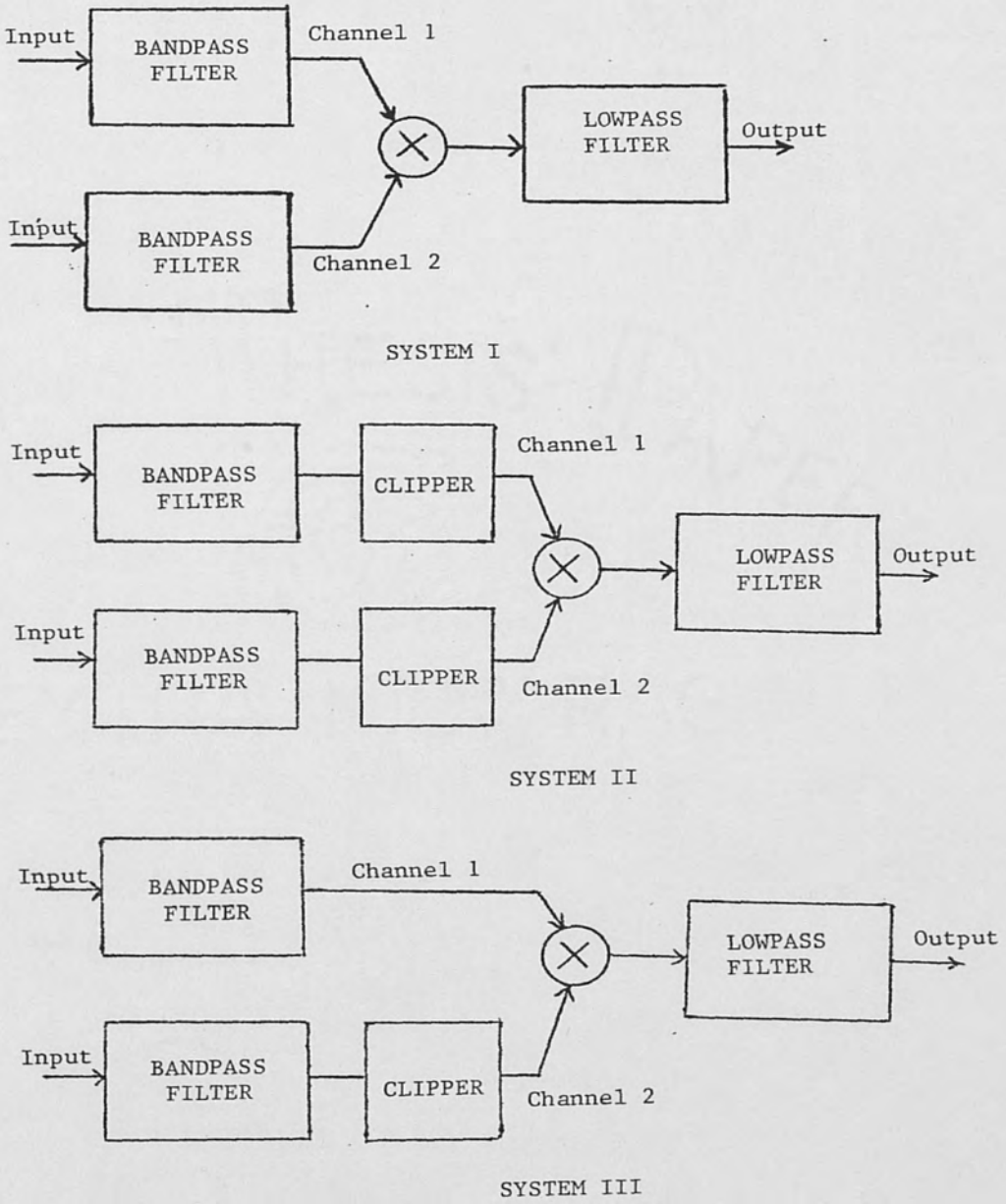

Fig. 1. Block diagrams of cross correlators

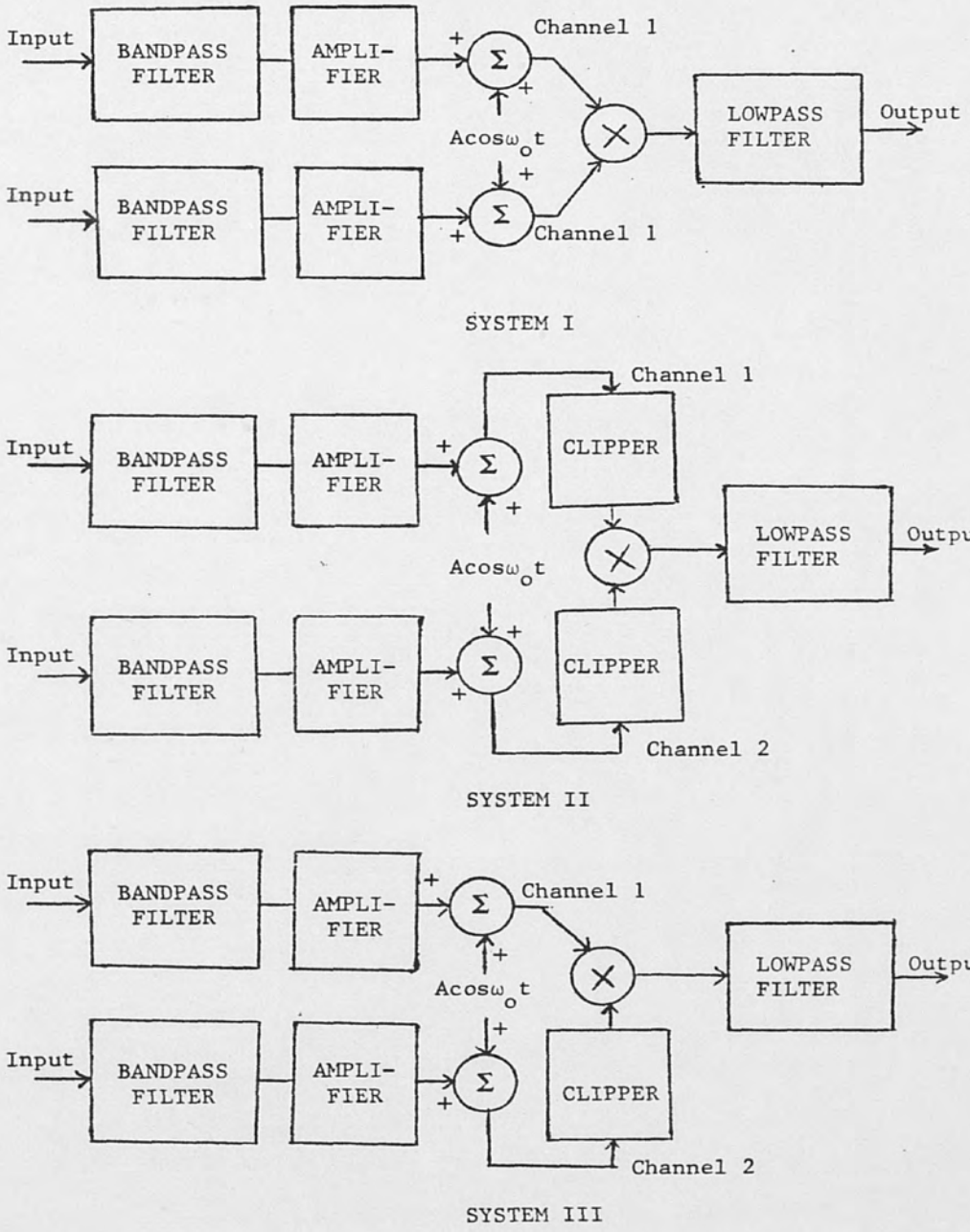

Fig. 2. Block diagrams of simulated cross correlators

II. THEORETICAL MODELS

The theoretical models of the standard analog correlator, the polarity coincidence correlator and the modified type of the polarity coincidence correlator are diagrammed in fig. 1. In all three correlators, it is assumed the inputs consist of sine waves of the same frequency ω_o, same amplitude A and zero relative phase angle, plus stationary Gaussian noise with means zero and variances σ_1^2 and σ_2^2 for channel 1 and channel 2 respectively. In all three systems, the noise terms are assumed independent. The outputs of the bandpass filters are given by

$$X_1(t) = A\cos\omega_o t + x_1(t)\cos\omega_o t - y_1(t)\sin\omega_o t$$
$$= R_1(t)\cos(\omega_o t + \theta_1(t)) \qquad (6)$$

and

$$X_2(t) = A\cos\omega_o t + x_2\cos\omega_o t - y_2\sin\omega_o t$$
$$= R_2(t)\cos(\omega_o t + \theta_2(t)), \qquad (7)$$

where the narrowband stationary Gaussian noise terms have been represented by Rice's decomposition (Rice 1944), $R_1(t)$ and $R_2(t)$ are the envelopes of the bandpass outputs, $\theta_1(t)$ and $\theta_2(t)$ are their random phases so that

$$R_1 = \left[(A + x_1)^2 + y_1^2\right]^{\frac{1}{2}}, \qquad (8)$$

$$\theta_1 = \arctan\left[y_1/(A + x_1)\right], \qquad (9)$$

$$R_2 = \left[(A + x_2)^2 + y_2^2\right]^{\frac{1}{2}} \qquad (10)$$

and

$$\theta_2 = \arctan\left[y_2/(A + x_2)\right]. \qquad (11)$$

Note that these variables are no longer represented as explicit functions of time as they vary slowly compared with the carrier due to the narrow bandwidth restriction. Therefore, the variables can be considered as constants with respect to time.

A. System I

After the bandpass outputs have been multiplied and lowpass filtered, the output of System I is given by

$$X_o(t) = \tfrac{1}{2}(A^2 + Ax_1(t) + Ax_2(t) + x_1(t)x_2(t) + y_1(t)y_2(t)) \tag{12}$$

The characteristic function C(t) for the random output $X_o(t)$ of the analog correlator has been derived by Andrews (1973). For the special case when the scaling factor K = 1, the correlation coefficient $\rho = 0$, the relative phase $\phi = 0$ and the signal amplitudes $A_1 = A_2 = A$, the characteristic function expression reduces to

$$C(t) = \frac{e(A)}{|M|^{\frac{1}{2}}} \frac{\exp\left[\dfrac{\gamma + i\beta t}{2(|W| + t^2/4)}\right]}{|W| + t^2/4} \tag{13}$$

where

$$e(A) = \exp\left[\frac{-A^2(\sigma_1^2 + \sigma_2^2)}{2\sigma_1^2\sigma_2^2}\right] \tag{14}$$

$$|M|^{\frac{1}{2}} = \frac{1}{|W|} = \sigma_1^2\sigma_2^2 \tag{15}$$

$$\beta = A^2|W| \tag{16}$$

$$\gamma = \beta(1/\sigma_1^2 + 1/\sigma_2^2) \tag{17}$$

Using the moment generating property of the characteristic function the first and second moments are obtained as

$$m_1 = -iC'(0) = A^2/2 \tag{18}$$

and

$$m_2 = -C''(0) = \tfrac{1}{2}\sigma_1^2\sigma_2^2(1 + S_1 + S_2) + m_1^2 \tag{19}$$

Substituting (18) and (19) in (5), the output SNR is

$$SNR_o = \frac{2S_1S_2}{1 + S_1 + S_2} \quad . \tag{20}$$

Hence, if the input SNRs are very small (S_1, S_2 <<1), then

$$SNR_o \cong 2S_1S_2 \tag{21}$$

and if input SNR of one channel is large (say channel 2, i.e., $S_2 >> S_1$, $S_2 >> 1$) the output SNR can be approximated as

$$SNR_o \cong 2S_1 \quad . \tag{22}$$

The solid curves in fig. 3 and 7 represent the plotting of the theoretical output SNR as a function of input SNRs for the analog cross-correlator.

B. System II

In this system, the clippers in the channels eliminate all amplitude information and retain only the polarity of the input signal relative to its mean value. The output $X_o(t)$ of the lowpass filter is given by (Andrews 1974)

$$X_o(t) = 1 - (2/\pi)\left|\theta_2(t) - \theta_1(t)\right| . \tag{23}$$

Relying upon the probability density function expression and the integral definition of moment, the first and second moments associated with the output of System II is given by (Andrews 1974)

$$m_1 = \frac{8}{\pi^2} \sum_{n=1}^{\infty} f(2n - 1; S_1)\, f(2n - 1; S_2)/(2n - 1)^2 \tag{24}$$

and

$$m_2 = \frac{1}{3} + \frac{4}{\pi^2} \sum_{n=1}^{\infty} f(2n; S_1)\, f(2n; S_2)/n^2 \tag{25}$$

where

$$f(n; S) = \frac{S^{n/2}}{n!}\, \Gamma(1 + n/2)\, {}_1F_1(n/2; 1 + n; -S) \tag{26}$$

The function $\Gamma(.)$ is the gamma function and ${}_1F_1\ (a;b;c)$ is the confluent hypergeometric function (Abramowitz 1965). Inserting the expressions of m_1 and m_2 in eq. (5), the output SNR_o can be calculated. Graphs of theoretical SNR_o for various input SNRs are shown in fig. 4 and 8 as solid curves. For the limiting cases of small input SNRs the output SNR can be approximated

$$SNR_o \cong \frac{12}{\pi^2} S_1 S_2 \text{ for } S_1,\ S_2 << 1. \tag{27}$$

C. System III

In this system the input amplitude of only one channel is clipped. This results in a reduction of the dynamic range of the multiplier as in System II without losing all amplitude information. The output behaves in some respects like that of a linear detector and is given by

$$X_o(t) = \frac{2R_1}{\pi} \cos\left[\theta_2(t) - \theta_1(t)\right]. \tag{28}$$

The characteristic function of the output X_o has been derived by Andrews (1980) and is given by

$$C(t) = e^{2\sigma_1{}^2 t^2/\pi^2} \sum_{n=0}^{\infty} \varepsilon_n f(n;\ S_2) I_n\left(\frac{2i\sigma_1 t}{\pi}\sqrt{2S_1}\right) \tag{29}$$

where

$$\varepsilon_n = \begin{cases} 1 & n = 0 \\ 2 & n \neq 0 \end{cases}$$

$$f(n;S_2) = \frac{S_2{}^{n/2}}{n!}\ \Gamma(1 + n/2)\ {}_1F_1(\tfrac{1}{2}n;\ n + 1;\ -S_2) \tag{30}$$

The function $I_n(\cdot)$ is the modified Bessel function of the first kind. It can be shown that $I_n(iz) = i^n J_n(z)$ where $J_n(z)$ is the

ordinary Bessel function of the first kind with index n. Using the characteristic function, the first two moments are readily found to be

$$m_1 = -iC'(o) = \sigma_1 (2S_1S_2/\pi)^{\frac{1}{2}} \; {}_1F_1(\tfrac{1}{2};\, 2;\, -S_2) \tag{31}$$

$$m_2 = -C''(o) = \frac{4\sigma_1^2}{\pi 2} \left[1 + S_1 + \tfrac{1}{2} S_1S_2 \; {}_1F_1(1;\, 3;\, -S_2)\right] . \tag{32}$$

By definition, the output SNR becomes

$$SNR_o = \frac{\{\tfrac{1}{2}\pi S_1S_2 \; e^{-S_2} \left[I_o(\tfrac{1}{2}S_2) + I_1(\tfrac{1}{2}S_2)\right]^2\}}{\{1 + S_1 + \frac{S_1}{S_2} (S_2 + e^{-S_2} - 1) - \tfrac{1}{2}\pi S_1S_2 \; e^{-S_2} \left[I_o(\tfrac{1}{2}S_2) + I_1(\tfrac{1}{2}S_2)\right]^2\}} \tag{33}$$

where we have used the following identities

$${}_1F_1(\tfrac{1}{2};\, 2;\, -S_2) = e^{-S_2/2}\left[I_o(\tfrac{1}{2}S_2) + I_1(\tfrac{1}{2}S_2)\right] \tag{34}$$

$${}_1F_1(1;\, 3;\, -S_2) = \frac{2}{S_2^2} (S_2 + e^{-S_2} - 1). \tag{35}$$

The asymptotic formulae for the output SNR are

$$SNR_o \cong \tfrac{1}{2}\pi S_1S_2 \qquad \text{for } S_1,\, S_2 \ll 1 \tag{36}$$

$$SNR_o \cong 2S_1 \qquad \text{for } S_2 \gg 1,\; S_2 \gg S_1 \tag{37}$$

Graphs of (33) are shown in fig. 5, 6, 9 and 10 for various values of input SNRs. The loss of symmetry between the two channels in this system is illustrated in the graphs.

III. EXPERIMENT

Special circuits were fabricated for each of the three cross-correlators utilizing standardized components which closely simulate idealized elements in an effort to verify the theoretical analysis on the three systems discussed in Section II. Fig. 2 shows simulated cross-correlators used to test experimentally the theoretical predictions. In each channel, the input consists of Gaussian noise with zero mean and frequency ranges up to 20 KHz. The Gaussian-distributed random noise was passed through a two-pole Butterworth bandpass filter with Q-factor of order of ten and unity gain. The center frequency of each filter was 2.1 KHz with a bandwidth of 200 Hz. Bandpass filters passed only those components whose frequencies were in a very narrow interval about the center frequency of the filter. Since the bandwidth of the filter is small compared to the carrier frequency, the output of the filter is called "narrowband" Gaussian noise and is represented by a sinusoidal wave with slowly varying random amplitude and phase (Rice 1944). The narrowband noise output of each bandpass filter was amplified and then summed with a sinusoidal signal having frequency 2 KHz and amplitude approximately 2 volts peak-to-peak. In System I the outputs of the summers which consist of signal plus narrowband noise components were multiplied

using a four quadrant integrated circuit multiplier. In System II the inputs were clipped by hard clippers prior to multiplication whereas in System III only one of the inputs was clipped. The multiplier output, which has an amplitude loss of 10, was then passed through a post-multiplier lowpass filter with a cutoff frequency set at the carrier frequency. The amplifier and the lowpass filter have a combined dc gain of 10 which compensates for the multiplier loss. The lowpass filter eliminates terms that have twice the carrier frequency or greater. In experimental set 1, the post-multiplier lowpass filter is a seventh-order Butterworth lowpass filter with a cutoff slope of 42 dB/octave, whereas in experimental set 2, we have a five-pole Chebyshev filter with a maximum loss of 1 dB in the passband. The electronic design of the circuits used in the fabrication of the cross-correlators is discussed in detail in Appendix 2. Magnitude plots of the transfer function of the bandpass filter and lowpass filters are also illustrated in Appendix 2.

Data was collected using a Digital Equipment Corporation Modular Instrument Computer (MINC). The computer was programmed to collect three thousand data points over a period of thirty seconds. The first and second statistical moments were then computed. The first two statistical moments of the output of the cross-correlators, the noise from channel 1, the noise from channel 2 and the signals were computed. Using equations (3), (4) and (5) the input SNRs and output SNR were then calculated. By keeping input SNR in one channel fixed and letting it vary in the other, the output SNR was computed

as a function of the input SNR in each channel. Plots of experimental and theoretical output SNRs for various values of input SNRs are shown in fig. 3 - 6 for set 1 and fig. 7 - 10 for set 2. In all cases the experimental data is in close agreement with the theoretical predictions.

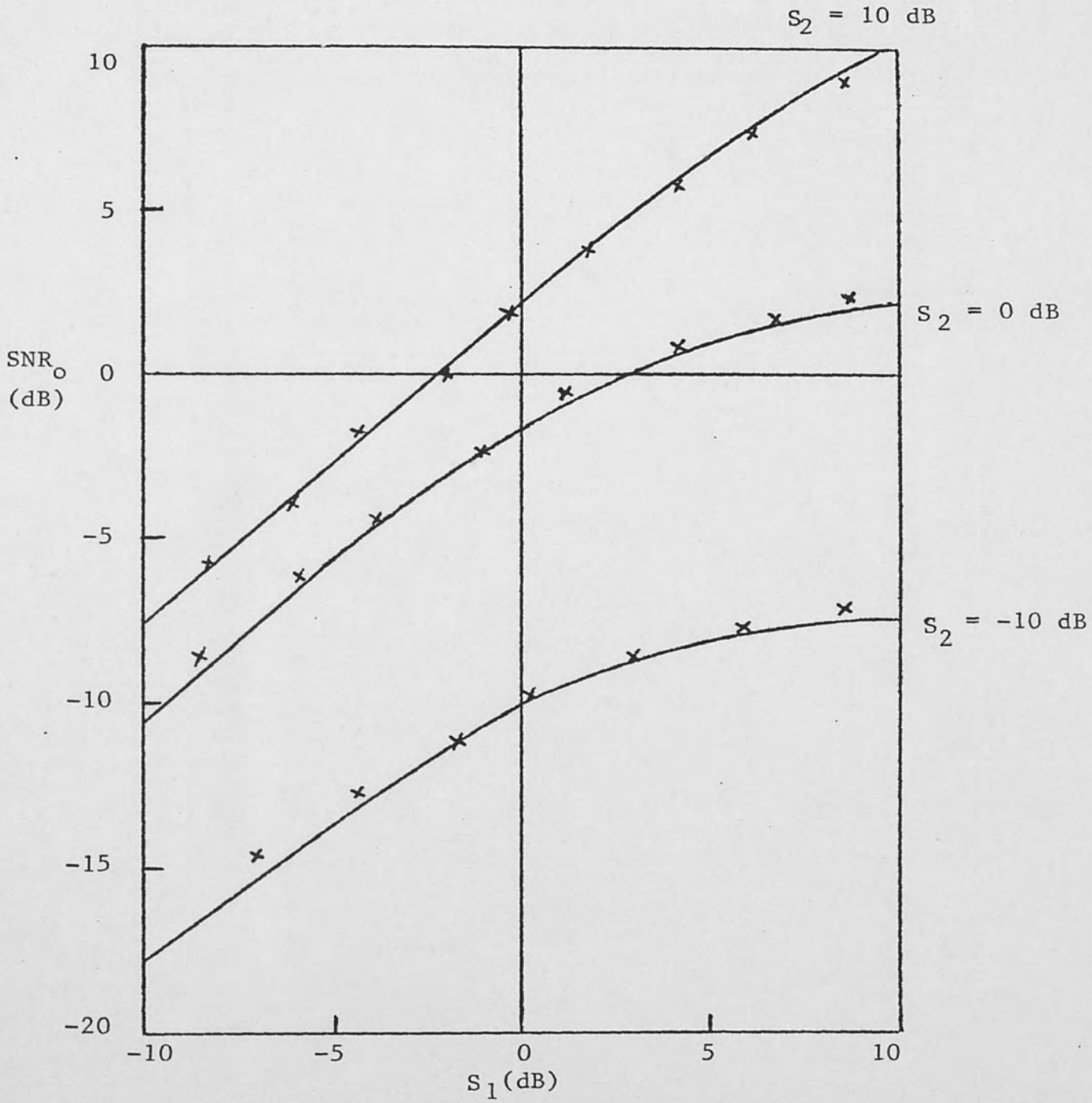

Fig. 3. (Set 1) Theoretical and experimental output SNR of System I. The postmultiplier lowpass filter is a seventh-order Butterworth lowpass filter. (The solid curves represent the theoretical values while the experimental values are denoted by a cross.)

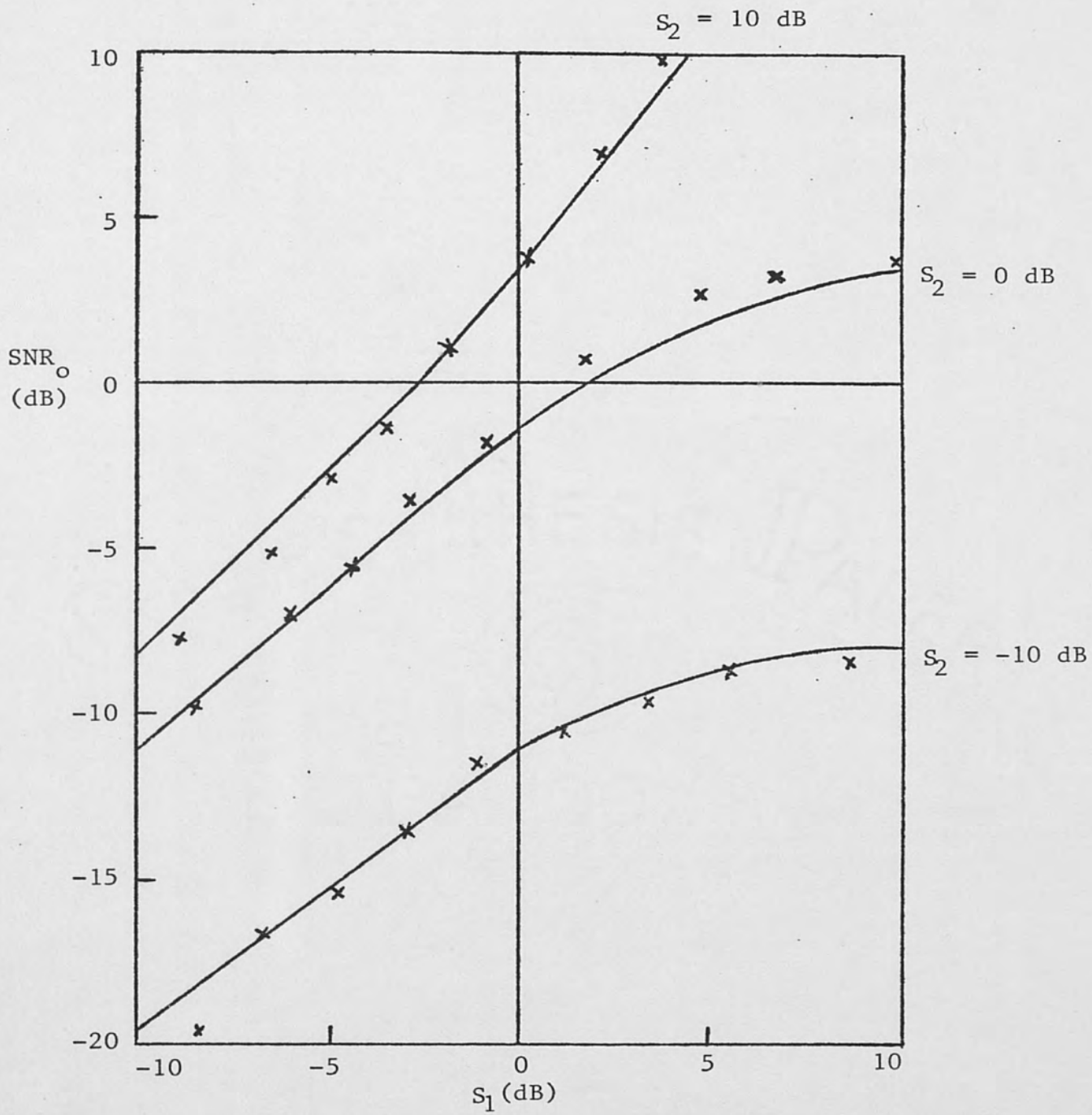

Fig. 4. (Set 1) Theoretical and experimental output SNR of System II. The postmultiplier lowpass filter is a seventh-order Butterworth lowpass filter. (The solid curves represent the theoretical values while the experimental values are denoted by a cross.)

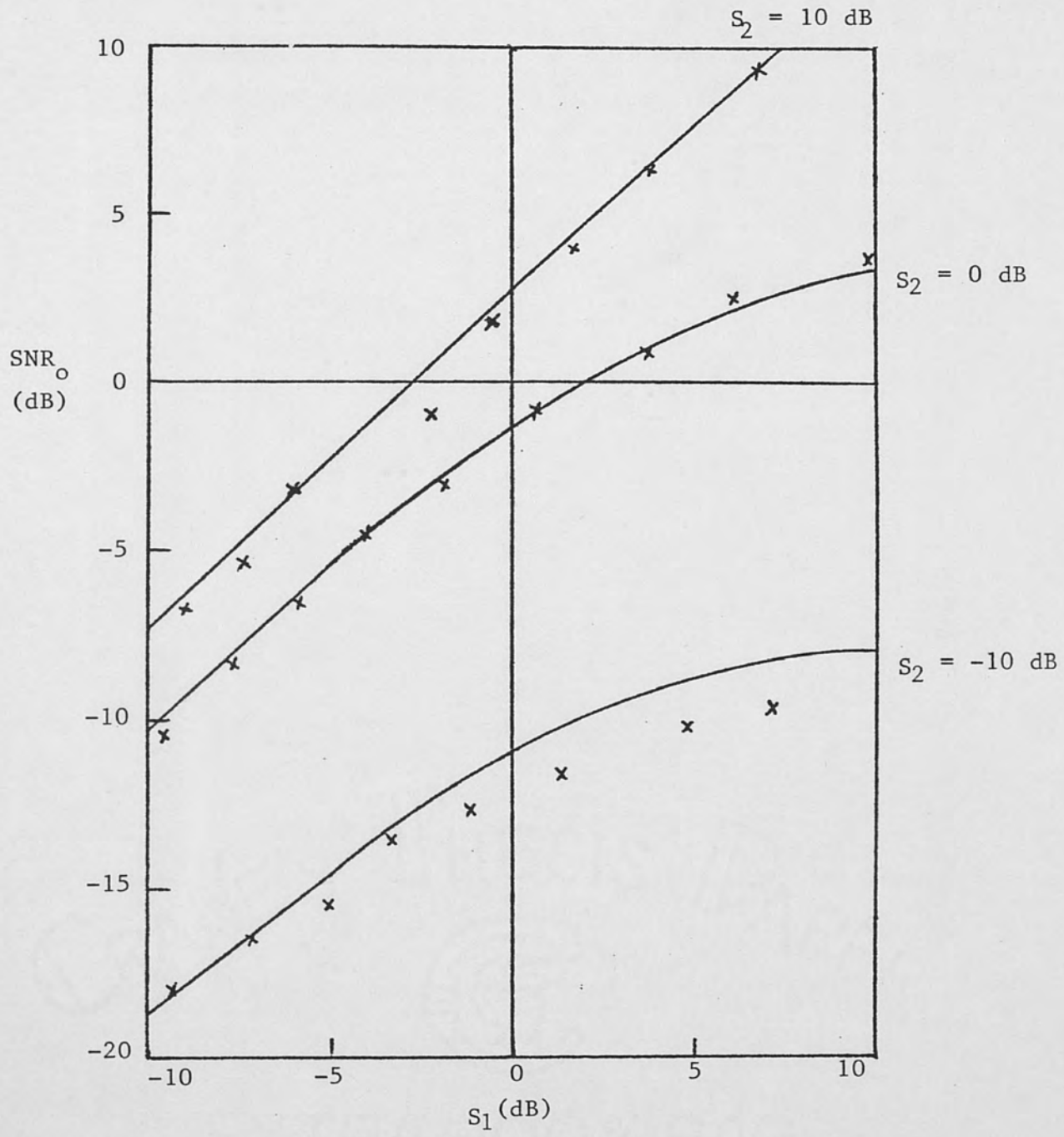

Fig. 5. (Set 1) Theoretical and experimental output SNR of System III. The postmultiplier lowpass filter is a seventh-order Butterworth lowpass filter. (The solid curves represent the theoretical values while the experimental values are denoted by a cross.)

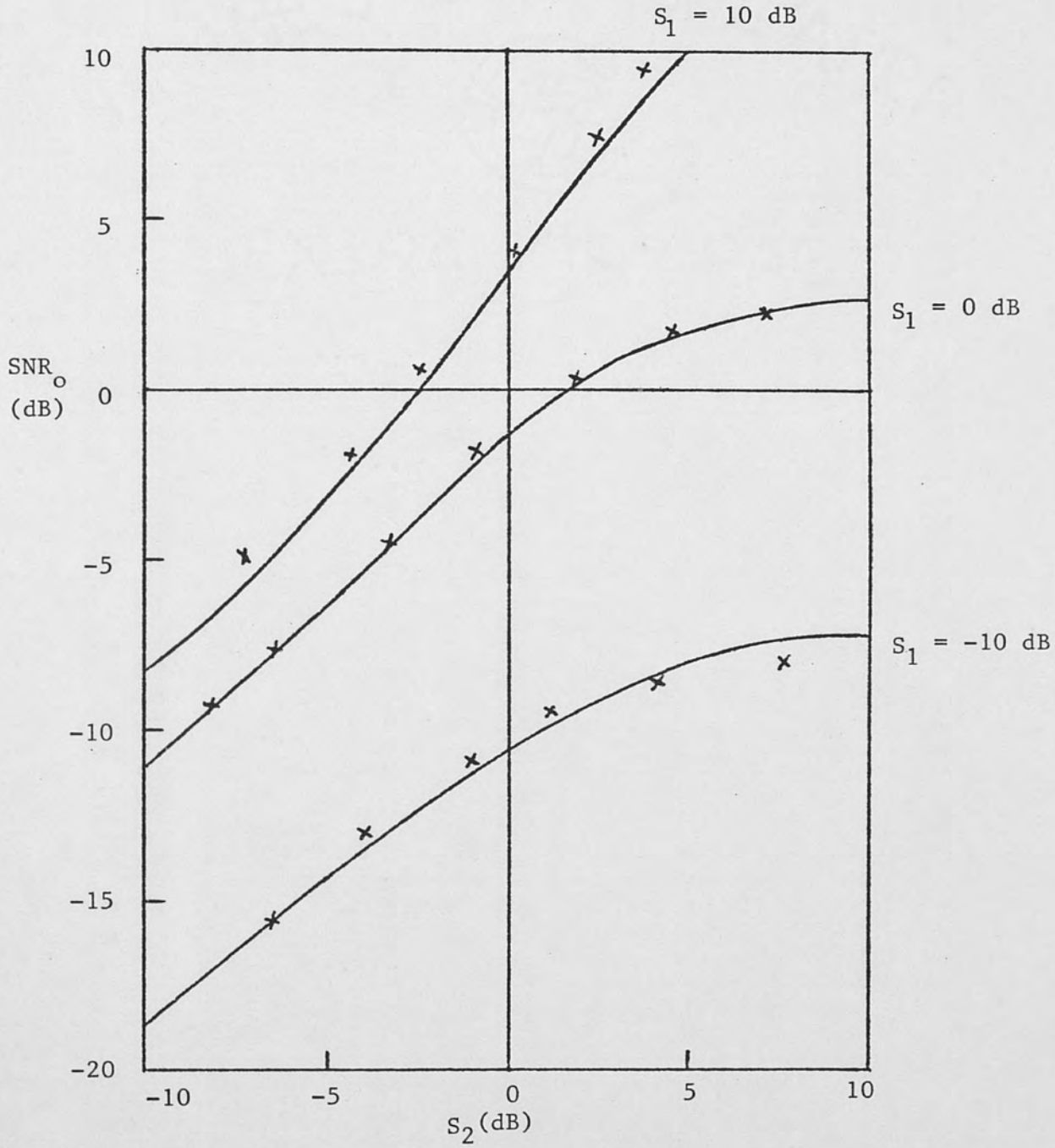

Fig. 6. (Set 1) Theoretical and experimental output SNR of System III. The postmultiplier lowpass filter is a seventh-order Butterworth lowpass filter. (The solid curves represent the theoretical values while the experimental values are denoted by a cross.)

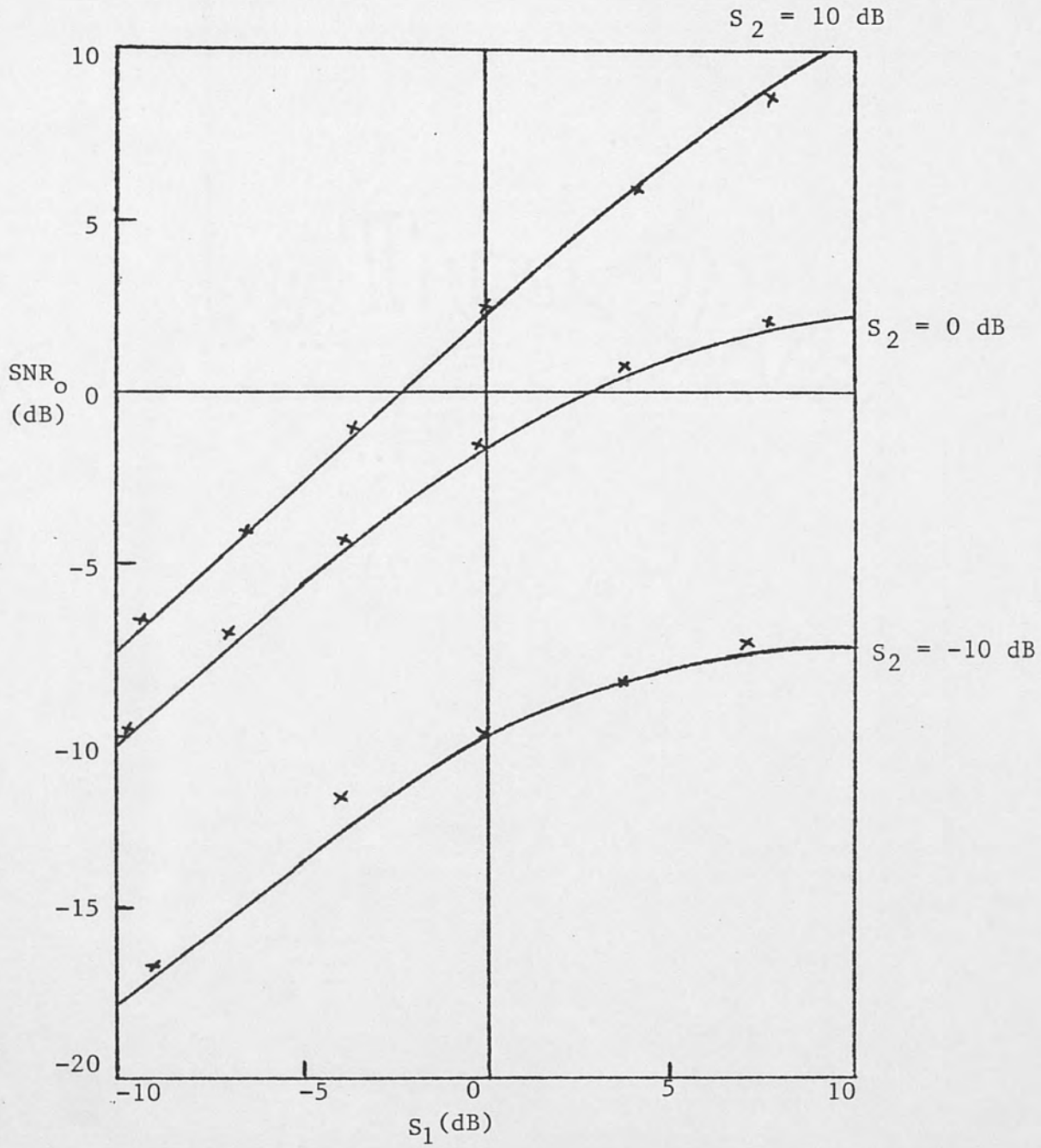

Fig. 7. (Set 2) Theoretical and experimental output SNR of System I. The postmultiplier lowpass filter is a five-pole Chebyshev lowpass filter with 1-dB ripple in the passband. (The solid curves represent the theoretical values while the experimental values are denoted by a cross.)

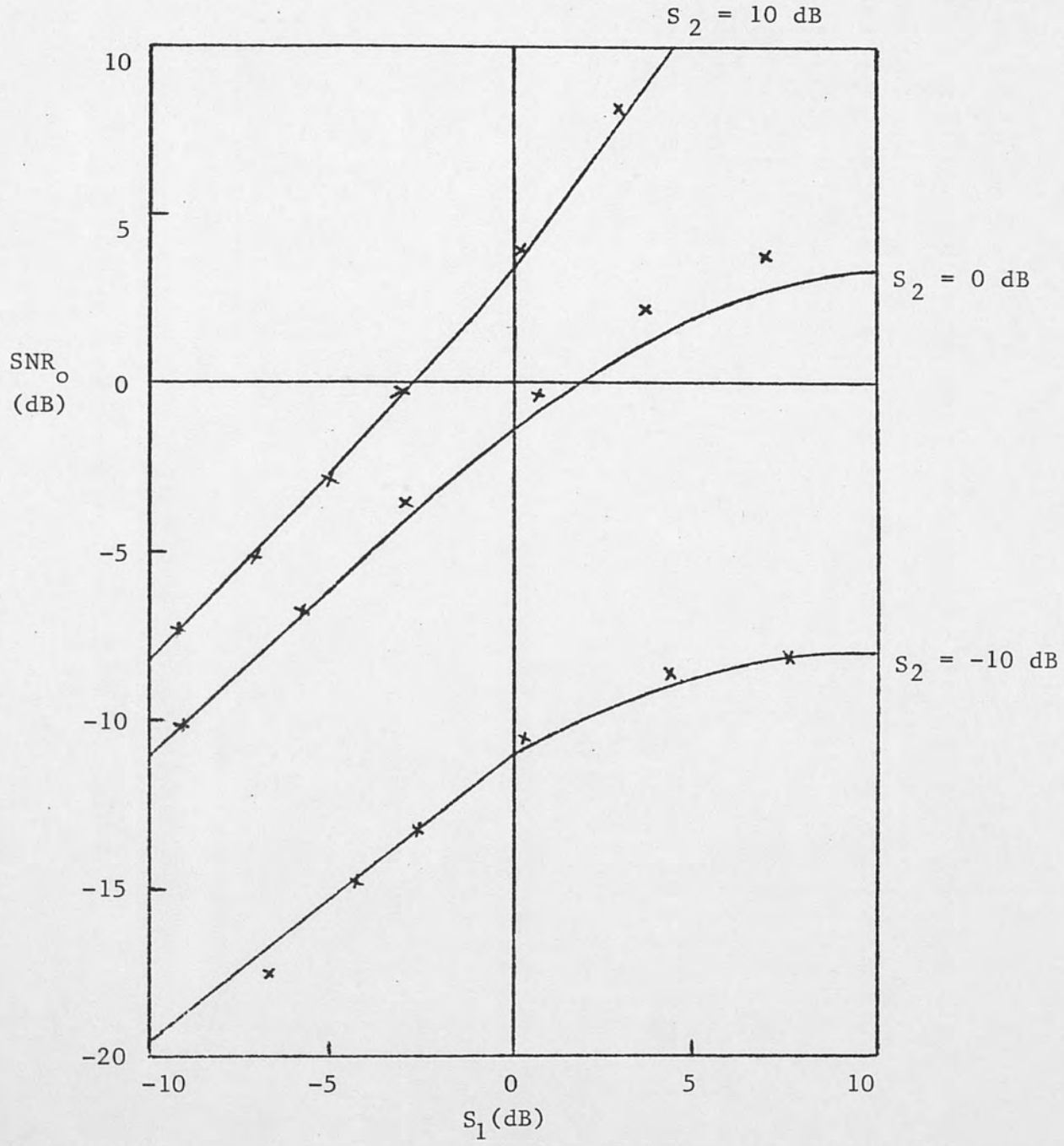

Fig. 8. (Set 2) Theoretical and experimental output SNR of System II. The postmultiplier lowpass filter is a five-pole Chebyshev lowpass filter with 1-dB ripple in the passband. (The solid curves represent the theoretical values while the experimetnal values are denoted by a cross.)

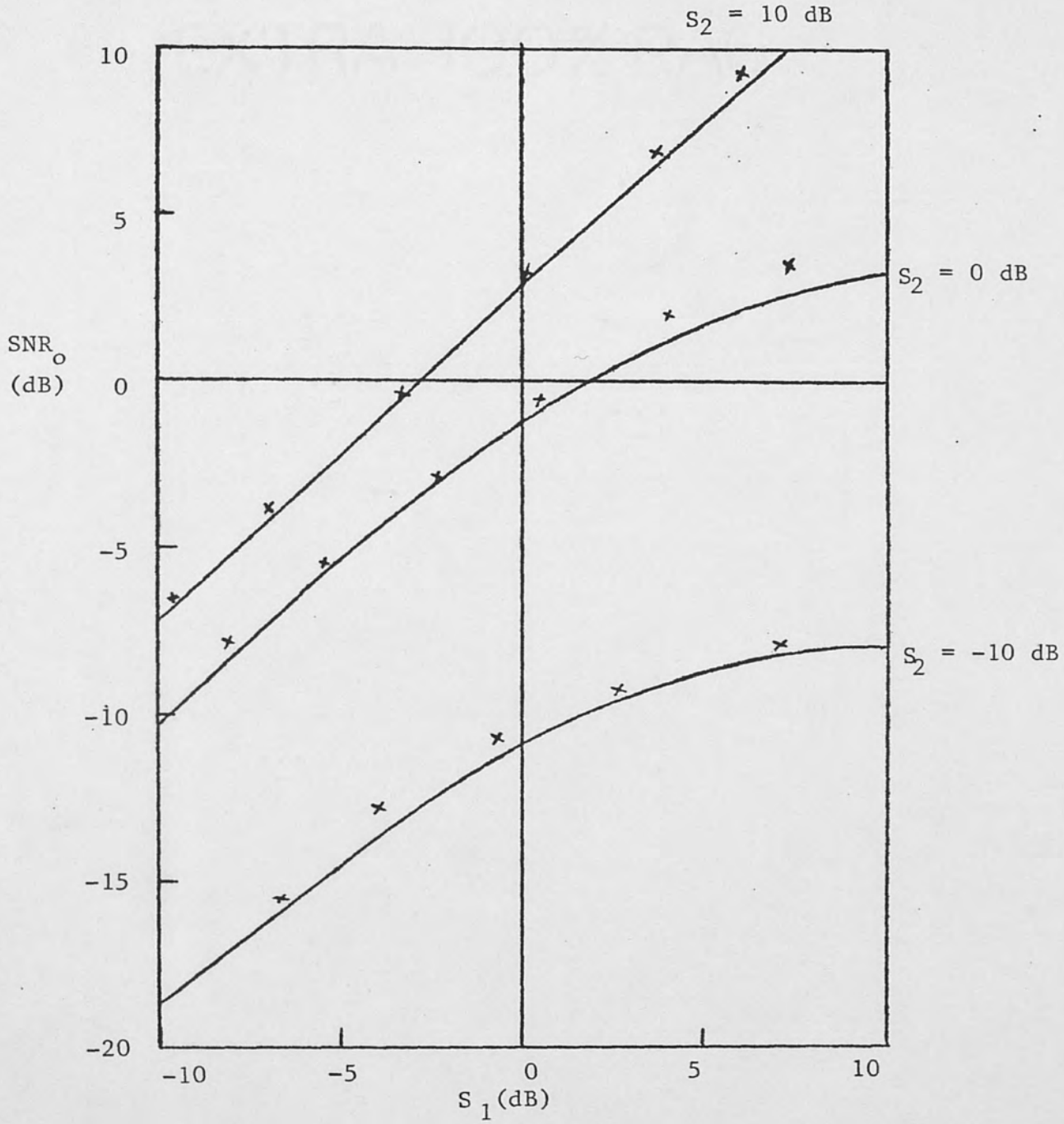

Fig. 9. (Set 2) Theoretical and experimental output SNR of System III. The postmultiplier lowpass filter is a five-pole Chebyshev lowpass filter with 1-dB ripple in the passband. (The solid curves represent the theoretical values while the experimental values are denoted by a cross.)

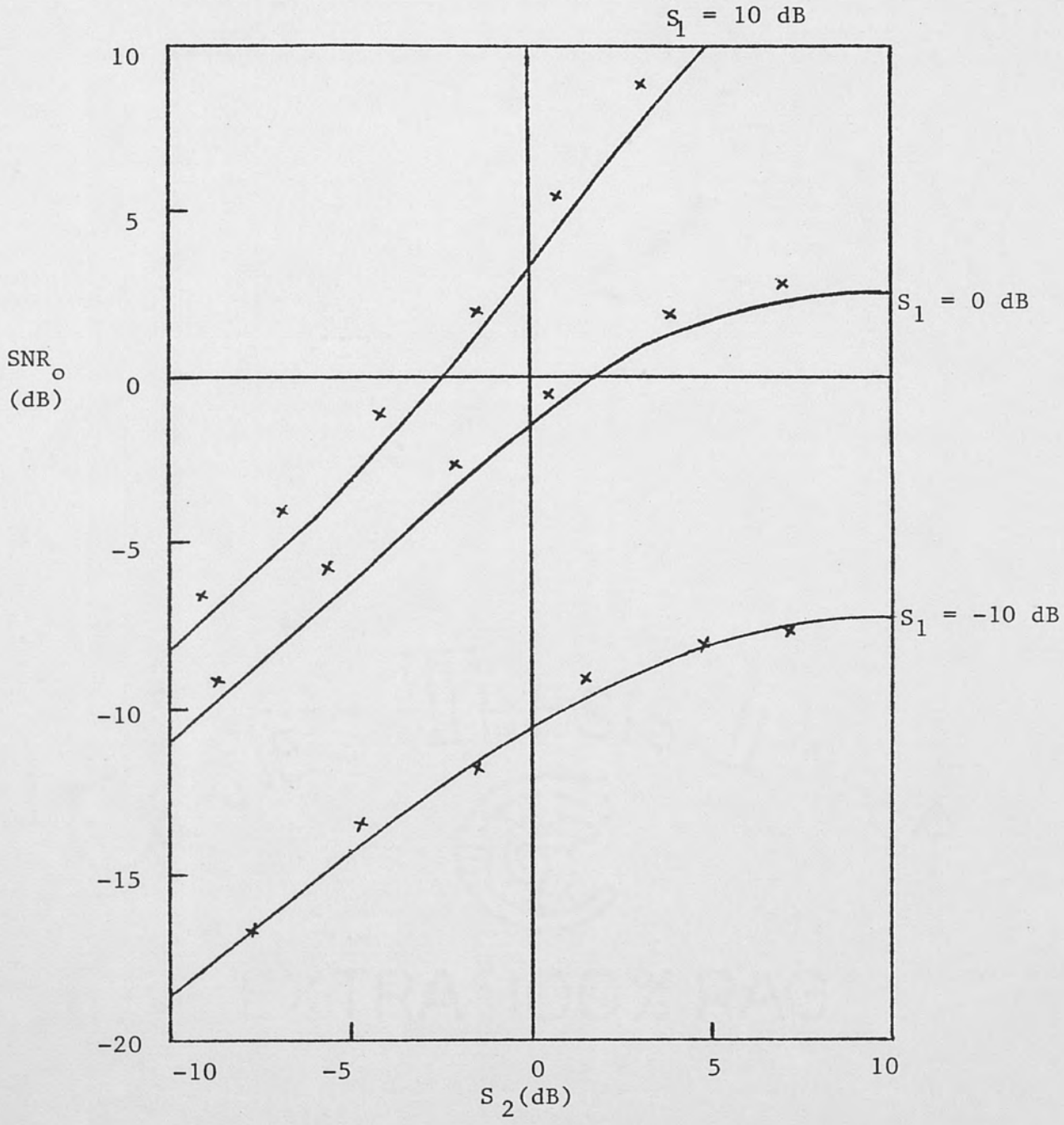

Fig. 10. (Set 2) Theoretical and experimental output SNR of System III. The postmultiplier lowpass filter is a five-pole Chebyshev lowpass filter with 1-dB ripple in the passband. (The solid curves represent the theoretical values while the experimental values are denoted by a cross.)

IV. CONCLUDING REMARKS

The results of the experimental measurements show that the theoretical models can be used to predict the output SNR (as a function of input SNR in each channel) accurately. The cross-correlator performances in terms of output SNRs are compared using fig. 11 and 12 and asymptotic formulae.

Of practical interest is the case when the input SNRs are much less than one; we found the analog correlator outperforms the polarity coincidence correlators. Specifically, there is approximately a 2 dB clipping loss in output SNR for System II as compared with System I. This result satisfies the condition obtained by Cheng (1968). Cheng shows that the maximum clipping loss in output SNR for the PCC with respect to the analog correlator is 4 dB. As expected, the System III exhibits only a 1 dB loss as compared with System I. Thus it is seen that the drop in output SNR for the PCC, which features a clipper in each channel, is more severe than that of System III which incorporates a clipper in only one channel. However, when one input SNR in one channel is large and the other is small the output SNR of all three systems is about 1 dB from each other. Also, the output SNRs of the polarity coincidence correlators can be several dB above that of the analog correlator when the input

SNRs are large.

A further comparison of all three systems is shown in fig. 12. Here the input SNR in each channel are assumed to be identical, i.e., $S_1 = S_2 = S$. We note that there exists a critical value of input SNR for which the output SNRs of all three systems are identical. If input SNR exceeds this critical value the output SNRs of System II and System III will be greater than the output SNR of System I. While making an extensive study on the comparison of PCC performance with respect to the analog correlator based upon output SNRs, Cheng (1968) has pointed out the existence of such a critical value. The mathematical expressions, graphs and asymptotic formulae simplify the task of a communication systems engineer in the selection of an optimum system in terms of the input SNRs only. In practice, since System II and System III result in a reduction of the complexity of hardware (hence a reduction in cost), the design engineer has to decide on a trade-off point between cost and performance.

Last but not least, we found that simulated cross-correlators with Chebyshev lowpass filters have higher output SNRs than systems with Butterworth lowpass filters for the same input SNRs. This is more distinctive in System II and System III. This may be contributed to the greater roll-off of the Chebyshev lowpass filter over the Butterworth lowpass filter and their fluctuations in the passbands. The finite roll-off of the output lowpass filters and the fluctuations in their passbands are the primary cause of the small discrepancy found from time to time between the theoretical curves

and experimental measurements. Even though the bandpass center frequency was 2.1 KHz instead of the desired 2 KHz, there was no significant error contributed to this shift in frequency.

Though this research report has successfully verified the theoretical models in all cases, it is in no way complete. Further investigation can be done in the following areas.

1. A theoretical derivation of mathematical expressions for output SNRs, characteristic functions, pdfs for System II and System III when the noise terms are correlated with correlation coefficient ρ.
2. A theoretical analysis on System III to find the maximum clipping loss incurred on output SNR of System III as compared with the analog correlator.
3. An experimental verification of all three theoretical models for cases when the noise terms are correlated.

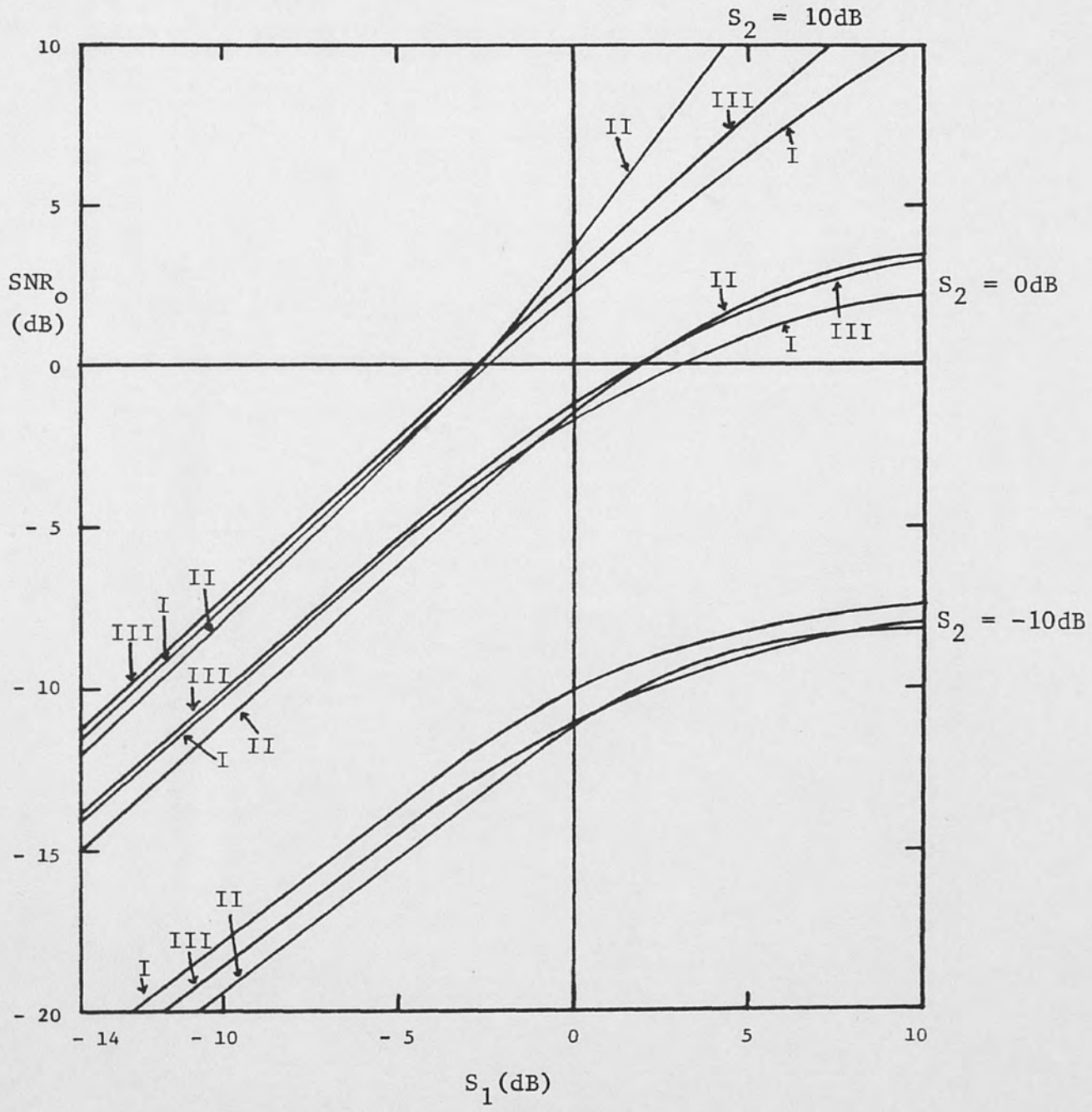

Fig. 11. A comparison of theoretical values of the output SNR for Systems I, II and III

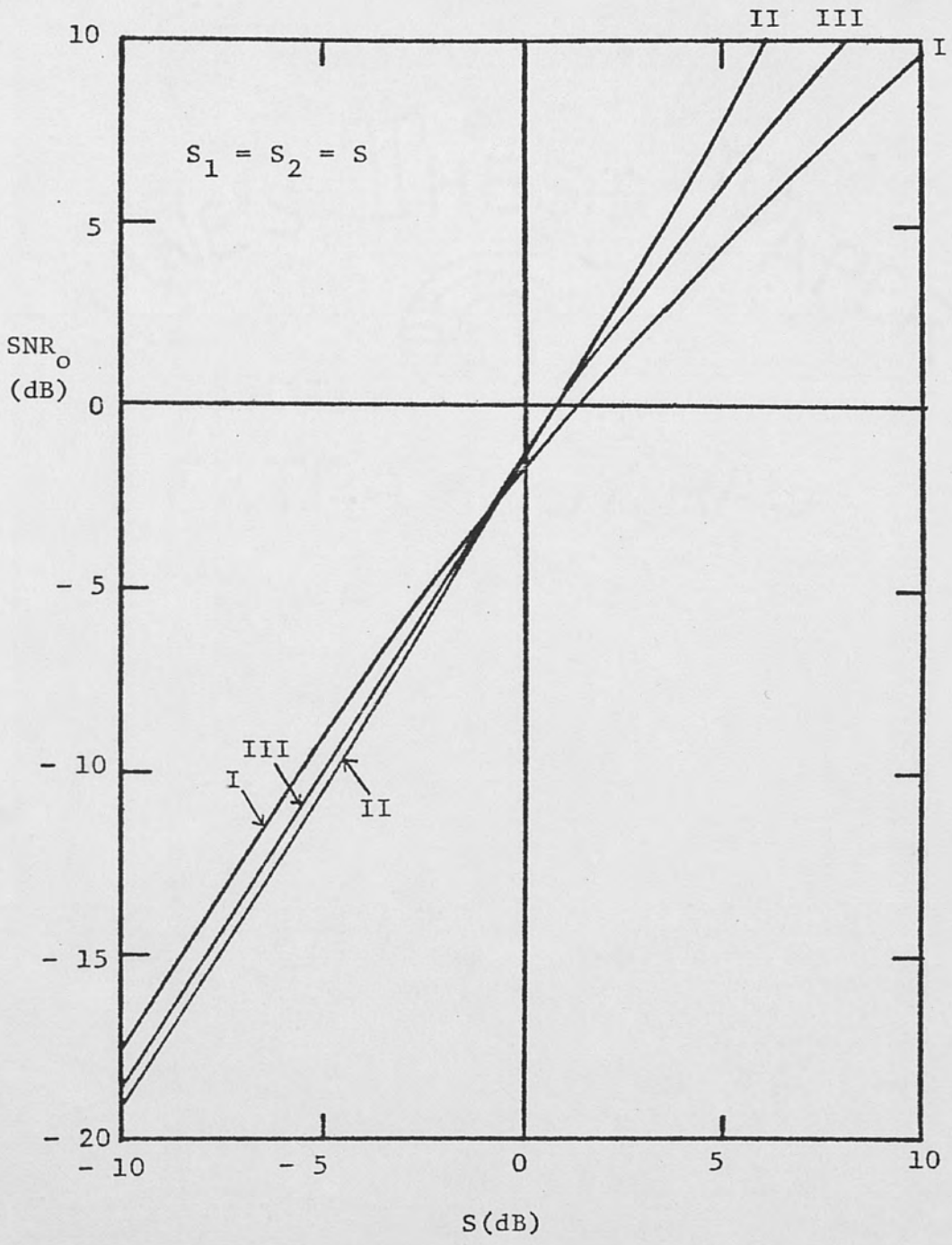

Fig. 12. A comparison of theoretical values of the output SNR for Systems I, II and III when the input SNR in each channel is the same

APPENDIX 1

LIST OF EQUIPMENT AND COMPONENTS

A. List of Equipments

1. 2 MHz function generator, Wavetek, model 182
2. Random-noise generators, General Radio Company, type 1390-B
3. Triple output power supply, Hewlett-Packard, type 6235A
4. Digital multimeter, Fluke, type 8000A
5. Oscilloscope, Tektronix, Inc., type 561B
6. Modular instrument computer, Digital Equipment Corporation, MINC-11

B. List of Components

1. LM-741CN operational amplifiers
2. LF-351N operational amplifiers
3. Burr-Brown universal active filters (UAF 31)
4. Analog devices multiplier AD533KH
5. Silicon diodes IN914
6. Resistors, capacitors, 5KΩ and 10KΩ potentiometers

APPENDIX 2

ELECTRONIC DESIGNS

In this appendix, design of electronic circuits that are used in the fabrication of the cross-correlators are discussed. The operational amplifiers (hereafter abbreviated as opamps) used in the following electronic designs are assumed to be ideal. The ideal opamp is assumed to have the following properties

1. The gain is infinite
2. The input impedance is infinite
3. The output impedance is zero

A. Inverting Amplifier

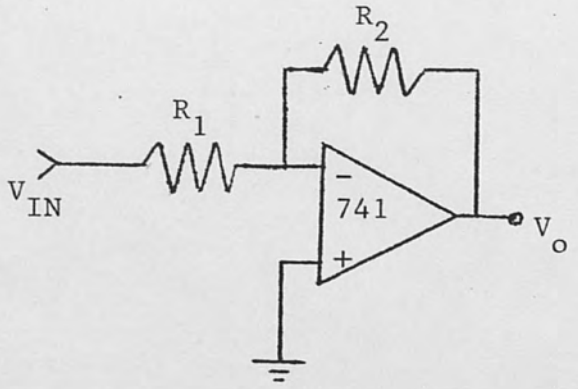

Fig. 2.1. Inverting operational amplifier

For the output voltage V_0 to be finite, the potential difference between the input terminals of the ideal opamp must be zero i.e.,

$$V_2 - V_1 = 0$$

Since V_2 is at ground potential, the voltage at the negative terminal is $V_1 = 0$. Using property (2) and summing the currents at node 1, we obtain

$$\frac{V_{IN} - V_1}{R_1} + \frac{V_0 - V_1}{R_2} = 0$$

substituting $V_1 = 0$ and simplifying gives

$$\frac{V_0}{V_{IN}} = -\frac{R_2}{R_1}$$

The inverting amplifier connection inverts the input voltage and scales it by a factor of $\frac{R_2}{R_1}$. Choosing $R_2 = R_1$, the output of the amplifier is just the inversion of the input.

B. Summing Amplifier

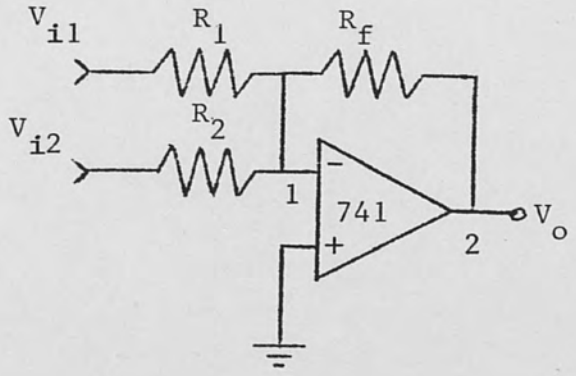

Fig. 2.2. Summing amplifier

Following the same reasoning as in part A, V_1 is at virtual ground. The currents can be determined as

$$I_{i1} = \frac{V_{i1}}{R_1}$$

$$I_{i2} = \frac{V_{i2}}{R_2}$$

$$I_f = \frac{V_0}{R_f}$$

As the input impedance of the opamp approaches infinity, the input current at the inverting input terminal of the amplifer approaches zero. Summing the currents at node 1, we get

$$\frac{V_{i1}}{R_1} + \frac{V_{i2}}{R_2} + \frac{V_0}{R_f} = 0$$

$$V_0 = -\frac{R_f}{R_1} V_{i1} - \frac{R_f}{R_2} V_{i2}$$

Choosing $R_f = R_1 = R_2$, the output of the amplifier is the inversion of the sum of the input voltages. A non-inverting summing amplifier can be obtained by passing this output through a basic inverting amplifier.

C. Bandpass Filter

To design a 2 pole Butterworth bandpass filter, with Q = 10, center frequency (f_c) = 2KHz and bandpass output-gain (A_{BP}) at f_c = 1.

A computer program to transform lowpass pole positions to bandpass pole positions is given in Appendix 3. Using the computer program the values of normalized natural frequency, f_n, and Q are 1.03600 and 14.15215 respectively. We will use the noninverting

input configuration to design the filter (Burr-Brown General Catalog 1979).

Since natural frequency (f_o) = 2 KHz x 1.03600 = 2.072 KHz (less than 8 KHz), the design equations are

1. $R_{F1} = R_{F2} = \frac{1.592 \times 10^8}{f_o}$

2. $A_{BP} = QA_{LP} = QA_{HP}$

3. $R_G = \frac{10^5}{A_{BP}} \frac{Q}{Q_P}$

4. $R_Q = \frac{10^5}{2Q_P - \frac{A_{BP}Q_P - 1}{Q}}$

$$R_{F1} = R_{F2} = \frac{1.592 \times 10^8}{2072} = 76.83K\Omega$$

Since f_oQ is less than 10^4 Hz, $Q = Q_P$

$R_G = 100\ K\Omega$

$R_Q = 3.802\ K\Omega$

Design Values	Experimental Measured Values
$R_{F1} = R_{F2} = 76.83\ K\Omega$	$R_{F1} = R_{F2} = 76.8\ K\Omega$
$R_G = 100\ K\Omega$	$R_G = 100\ K\Omega$
$R_Q = 3.802\ K\Omega$	$R_Q = 3.61\ K\Omega$

A plot of $|V_0/V_{IN}|$ versus frequency is shown in fig. 2.9. The circuit for the required filter is shown below

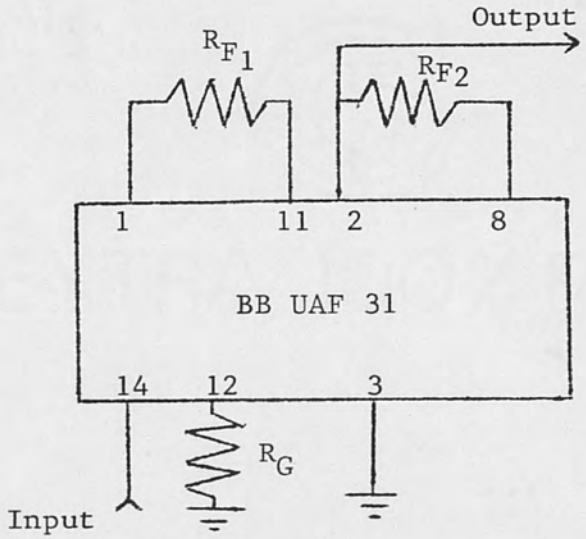

Fig. 2.3. Bandpass filter circuit

The noninverting input configuration for a bandpass filter results in an inverted output.

D. Lowpass Chebyshev Filter

To synthesize a lowpass filter with the following specifications

1. Cutoff frequency, f_p = 2000 Hz
2. Stopband frequency, f_s = 4000 Hz
3. Maximum passband loss, A max = 1 dB
4. Minimum stopband loss, A min = 40 dB
5. dc gain = 0 dB

The normalized stopband edge frequency is $\Omega_s = \frac{f_s}{f_p} = \frac{4000}{2000} = 2.$ Therefore, the required order is 5 (Daryanani 1976). The normalized Chebyshev lowpass function $T_N(s)$, is

$$T_N(s) = \frac{0.12283}{(s^2 + 0.17892s + 0.98831)} \cdot \frac{1}{(s^2 + 0.46841s + 0.42930)} \cdot \frac{1}{(s + 0.28949)}$$

Since f_p = 2000 Hz; W_p = 12566.371 rad./sec. The desired fifth-order lowpass filter function $T_{LP}(s)$ is obtained by denormalizing $T_N(s)$ by replacing s by s/12566.371

$$T_{LP}(s) = \frac{3.8491 \times 10^{19}}{(s^2 + 2248.3751s + 1.5607 \times 10^8)} \cdot \frac{1}{(s^2 + 5886.2138s + 6.7792 \times 10^7)} \cdot \frac{1}{(s + 3637.8387)}$$

$$T_{LP}(s) = \frac{k_1}{(s^2 + 2248.3751s + 1.5607 \times 10^8)} \cdot \frac{k_2}{(s^2 + 5.8862 \times 10^3 s + 6.7792 \times 10^7)} \cdot \frac{k_3}{(s + 3.6378 \times 10^3)}$$

where $k_1k_2k_3 = 3.8491 \times 10^{19}$

Stage 1

$$T_{LP1}(s) = \frac{2.0809 \times 10^8}{(s^2 + 2.2484 \times 10^3 s + 1.5607 \times 10^8)}$$

Here $k_1 = 2.0809 \times 10^8$ has been chosen so that $k_1 = 4/3$ when s = 0.

Compare $T_{LP1}(s)$ with the standard lowpass functions

$$T_{LPs}(s) = \frac{k}{(s^2 + \frac{W_p}{Q_p} s + W_p^2)}$$

$k = 2.0809 \times 10^8$ $\quad$ $W_p/Q_p = 2.2484 \times 10^3$ $\quad$ $W_p^2 = 1.5607 \times 10^8$

$W_p = 1.2493 \times 10^4$ $\quad$ $Q_p = 5.5563$

To realize the above transfer function we use the Saraga design of the Sallen and Key circuit (Daryanani 1976). The element values proposed by Saraga are

$C_2 = 1$ $\quad C_1 = 1.7321\ Q_p$ $\quad R_2 = \frac{1}{1.7321\ W_p}$ $\quad R_1 = \frac{1}{Q_p W_p}$ $\quad k = 4/3$

Substituting the values of W_p and Q_p, we get

$C_{21} = 1$ $\quad C_{11} = 9.6238$ $\quad R_{21} = 4.6214 \times 10^{-5}$ $\quad R_{11} = 1.4406 \times 10^{-5}$

To obtain practical element values, multiply the resistors by 10^9 and divide the capacitors by 10^9 then

$C_{21} = .001\ \mu F$ $\quad C_{11} = .0096\ \mu F$ $\quad R_{21} = 46.21\ k\Omega$ $\quad R_{11} = 14.41\ k\Omega$

The term $k = \frac{4}{3} = 1 + \frac{r_{21}}{r_{11}}$ can be realized using $r_{21} = 10\ k\Omega$ and $r_{11} = 30\ k\Omega$.

Stage 2

$$T_{LP2}(s) = \frac{9.0389 \times 10^7}{s^2 + 5886.2s + 6.7792 \times 10^7}$$

Here $k_2 = 9.0389 \times 10^7$ has been chosen so that $k_2 = 4/3$ when $s = 0$. Compare $T_{LP}(s)$ with the standard lowpass function, we get

$k = 9.0389 \times 10^7$ $\quad W_p/Q_p = 5.8862 \times 10^3$ $\quad W_p^2 = 6.7792 \times 10^7$

$W_p = 8.2336 \times 10^3$ $\quad Q_p = 1.3988$

As in stage 1, using these values of W_p and Q_p, the element values of the Saraga design are

$C_{22} = 1$ $\quad C_{12} = 2.4228$ $\quad R_{22} = 7.012 \times 10^{-5}$

$R_{12} = 8.6827 \times 10^{-5}$

On impedance scaling by a factor of 10^9 we get the practical value of elements.

$C_{22} = .001\ \mu F$ $\quad C_{12} = .0024\ \mu F$ $\quad R_{22} = 70.12\ k\Omega$ $\quad R_{12} = 86.8\ k\Omega$

Choose r_{22} = 10 kΩ and r_{12} = 30 kΩ to realize the term k = 4/3.

Stage 3

$$T_{LP3}(s) = \frac{2.0464 \times 10^3}{s + 3.6378 \times 10^3}$$

The circuit below can be used to realize the above transfer function.

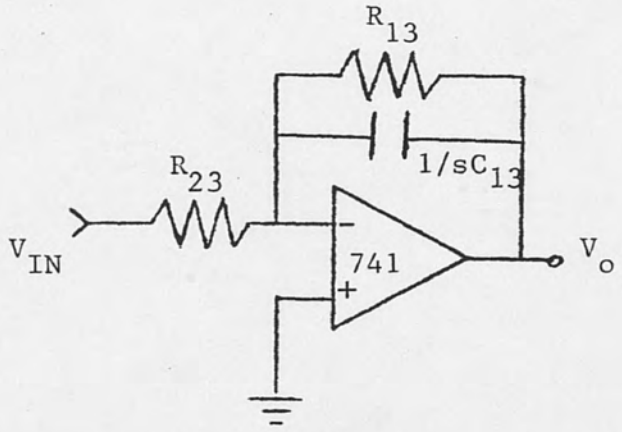

Fig. 2.4. Leaky Integrator

Analyzing the leaky integrator circuit shown, the transfer function is

$$\frac{V_0}{V_{IN}} = - \frac{\frac{1}{R_{23}C_{13}}}{s + \frac{1}{R_{13}C_{13}}}$$

Matching the coefficient of the two transfer functions gives

$$\frac{1}{R_{23}C_{13}} = 2.0464 \times 10^3$$

$$\frac{1}{R_{13}C_{13}} = 3.6378 \times 10^3$$

Choose C_{13} = 1, then $R_{23} = 4.8866 \times 10^{-4}$ $R_{13} = 2.7489 \times 10^{-4}$

Multiply the resistors by 10^8 and divide the capacitor by 10^8 yield

practical element values. Then

C_{13} = .01 μF $\quad R_{23}$ = 48.86 kΩ $\quad R_{13}$ = 27.49 kΩ

Below is the overall circuit of the filter.

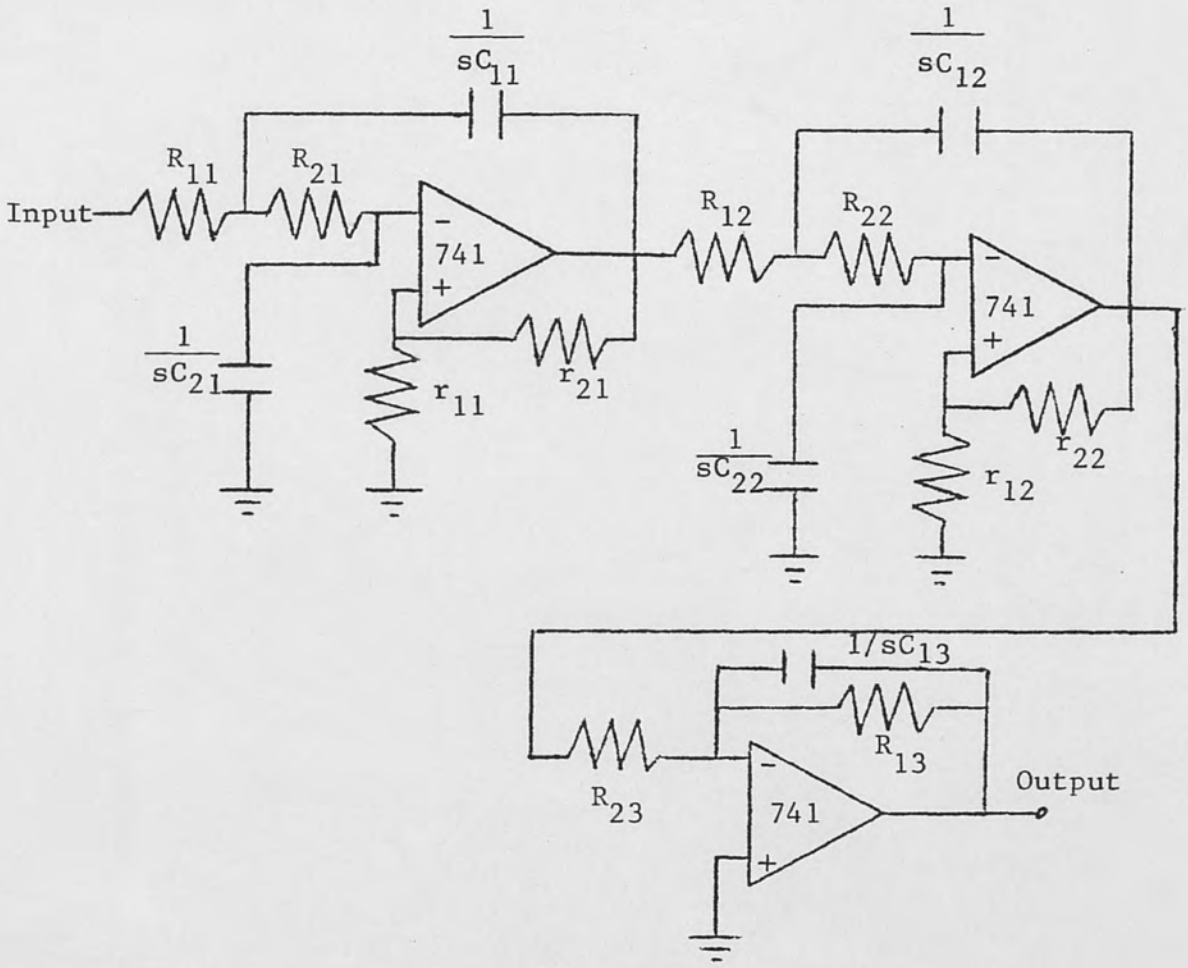

Fig. 2.5. Overall circuit of the fifth-order lowpass Chebyshev filter with A max = 1 dB

Note that the component R_{21} of stage 1 has been adjusted to 49.6 kΩ so that the filter will exhibit the desired performance. A plot of $|V_0/V_{IN}|$ of the filter versus $\log_{10} f$ is shown in fig. 2.10.

E. Lowpass Butterworth Filter

To synthesize a seventh-order Butterworth lowpass filter having a cut off frequency of 2 KHz and dc gain = 0 dB.

The denormalized transfer function of the lowpass filter is

$$T_{LP}(s) = \frac{4.9481 \times 10^{28}}{(s + 12566.371)(s^2 + 5592.563s + 1.579 \times 10^8)} \cdot \frac{1}{(s^2 + 15670.013s + 1.5791 \times 10^8)} \cdot \frac{1}{(s^2 + 22643.82s + 1.5791 \times 10^8)}$$

$$= \frac{k_1}{(s + 12566.371)} \cdot \frac{k_2}{(s^2 + 5592.563s + 1.579 \times 10^8)} \cdot \frac{k_3}{(s^2 + 15670.013s + 1.579 \times 10^8)} \cdot \frac{k_4}{(s^2 + 22643.82s + 1.579 \times 10^8)}$$

where $k_1k_2k_3k_4 = 4.9481 \times 10^{28}$ and $k_2 = k_3 = k_4 = 4/3$ for $s = 0$

Therefore $k_2 = k_3 = k_4 = 2.1055 \times 10^8$ and $k_1 = 5.3012 \times 10^3$

Stage 1

The transfer function of the first stage is

$$T_{LP1}(s) = \frac{5.3012 \times 10^3}{s + 12566.371}$$

As before in part D, the leaky integrator circuit can be used to realize this transfer function by choosing

$$\frac{1}{R_{11}C_{11}} = 12566.371 \qquad \frac{1}{R_{21}C_{11}} = 5.3012 \times 10^3$$

Letting $C_{11} = 1$, then $R_{11} = 7.958 \times 10^{-5}$; $R_{21} = 1.8864 \times 10^{-4}$

To obtain practical element values, the elements are impedance

scaled by 10^8 to yield

$C_{11} = .01\ \mu F \qquad R_{11} = 7.958\ k\Omega \qquad R_{21} = 18.864\ k\Omega$

Stage 2

The transfer function of the second stage is

$$T_{LP2}(s) = \frac{2.1055 \times 10^8}{s^2 + 5592.563s + 1.579 \times 10^8}$$

Compare with the standard lowpass transfer function

$$T_{LPs} = \frac{k}{s^2 + \frac{W_p}{Q_p} s + W_p^2}$$

we have $k = 2.1055 \times 10^8 \quad \frac{W_p}{Q_p} = 5592.563 \quad W_p^2 = 1.579 \times 10^8$

$W_p = 12566 \qquad Q_p = 2.247$

As in part D, using the Saraga design of the Sallen and Key circuit, the element values are

$C_{22} = 1 \qquad C_{12} = 3.892 \qquad R_{22} = 4.594 \times 10^{-5}$

$R_{12} = 3.542 \times 10^{-5} \qquad k = 4/3$

These elements are impedance scaled by 10^9 to yield

$C_{22} = .001\ \mu F \qquad C_{12} = .0039\ \mu F \qquad R_{22} = 45.94\ k\Omega$

$R_{12} = 35.42\ k\Omega \qquad r_{22} = 10\ k\Omega \qquad r_{12} = 30\ k\Omega$

Stage 3

The transfer function of the third stage is

$$T_{LP3}(s) = \frac{2.1055 \times 10^8}{s^2 + 15670.013s + 1.579 \times 10^8}$$

As in stage 2, the element values of the Saraga design are

$C_{23} = 1 \qquad C_{13} = 1.39 \qquad R_{23} = 4.59 \times 10^{-5}$

$R_1 = 9.92 \times 10^{-5} \qquad k = 4/3$

These elements are impedance scaled by a factor 2×10^8 to yield

$C_{23} = .005\ \mu F \quad C_{13} = .0069\ \mu F \quad R_{23} = 9.19\ k\Omega \quad R_{13} = 19.85\ k\Omega$

Again the term $k = 1 + r_{23}/r_{13} = 4/3$ can be realized by choosing $r_{23} = 10\ k\Omega$ and $r_{13} = 30\ k\Omega$

Stage 4

The transfer function for the fourth stage is

$$T_{LP4}(s) = \frac{2.1055 \times 10^8}{s^2 + 22643.82s + 1.579 \times 10^8}$$

Following the same procedure as in the previous two stages, the Saraga design element values are

$C_{24} = 1 \quad C_{14} = .961 \quad R_{24} = 4.594 \times 10^{-5} \quad R_{14} = 1.434 \times 10^{-4}$

$k = 4/3$

On impedance scaling by 2×10^8, the practical value of elements are

$C_{24} = .005\ \mu F \quad C_{14} = .0048\ \mu F \quad R_{24} = 9.19\ k\Omega$

$R_{14} = 28.68\ k\Omega \quad r_{24} = 10\ k\Omega \quad r_{14} = 30\ k\Omega$

The overall circuit of the filter is shown below.

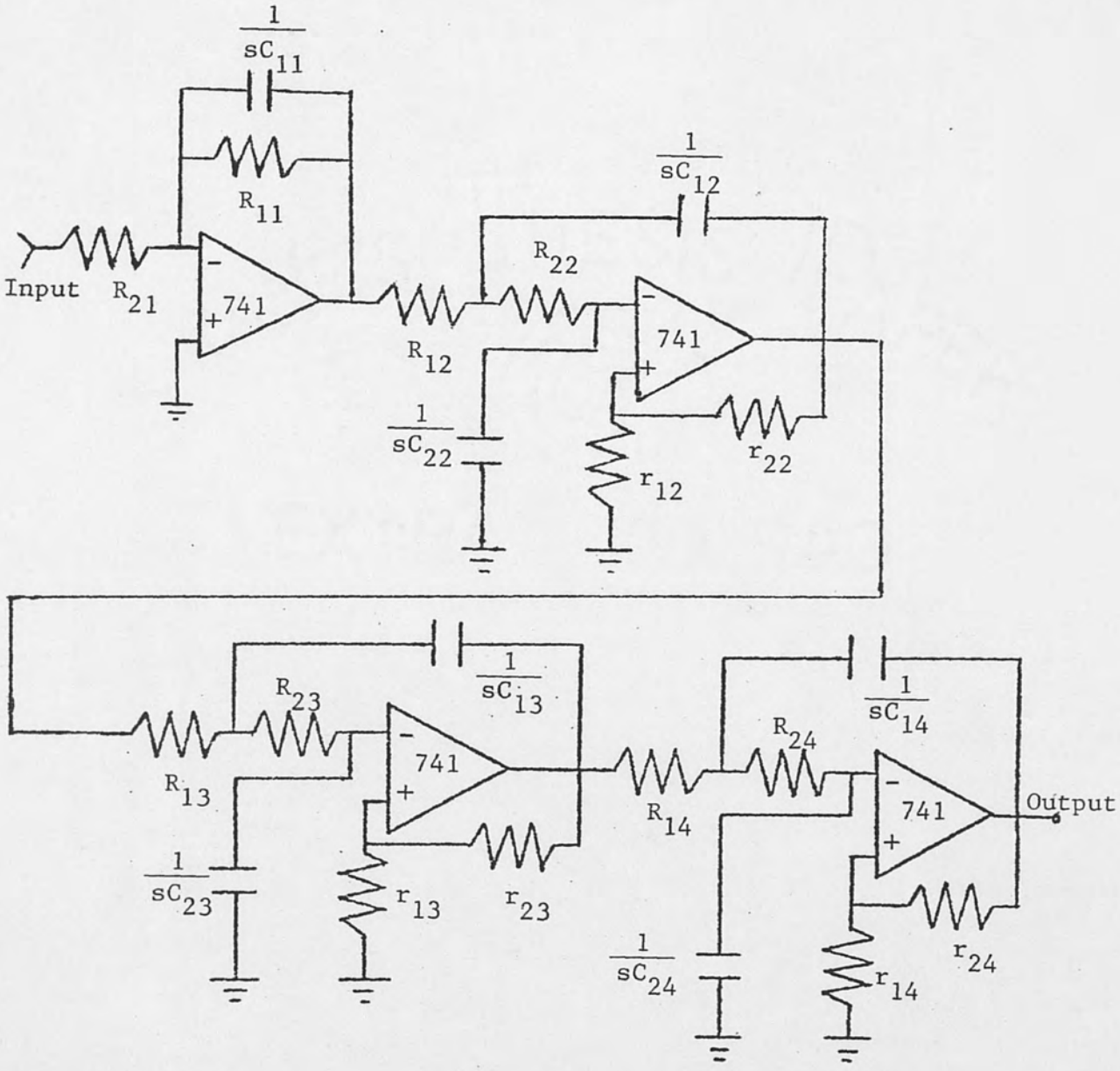

Fig. 2.6. Overall circuit of the seventh-order Butterworth lowpass filter

A plot of $\left|\frac{V_0}{V_{IN}}\right|$ versus $\log_{10} f$ is shown in fig. 2.11.

F. Amplitude Clipper

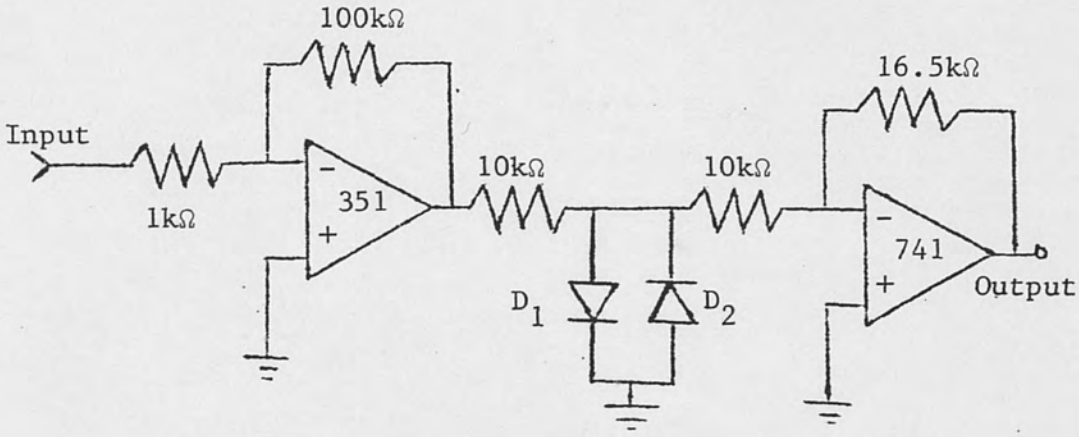

Fig. 2.7. Amplitude clipper

Essentially, the first section of the circuit is an inverting comparator whose output voltage is limited to the diode voltage (±.6 volt for silicon diodes). This diode voltage is then amplified to ±1 volt by the inverting amplifier. Fig. 2.8 shows the clipping of a sine wave.

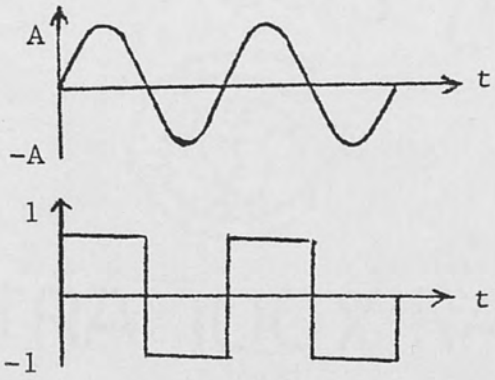

Fig. 2.8. A clipped sine wave

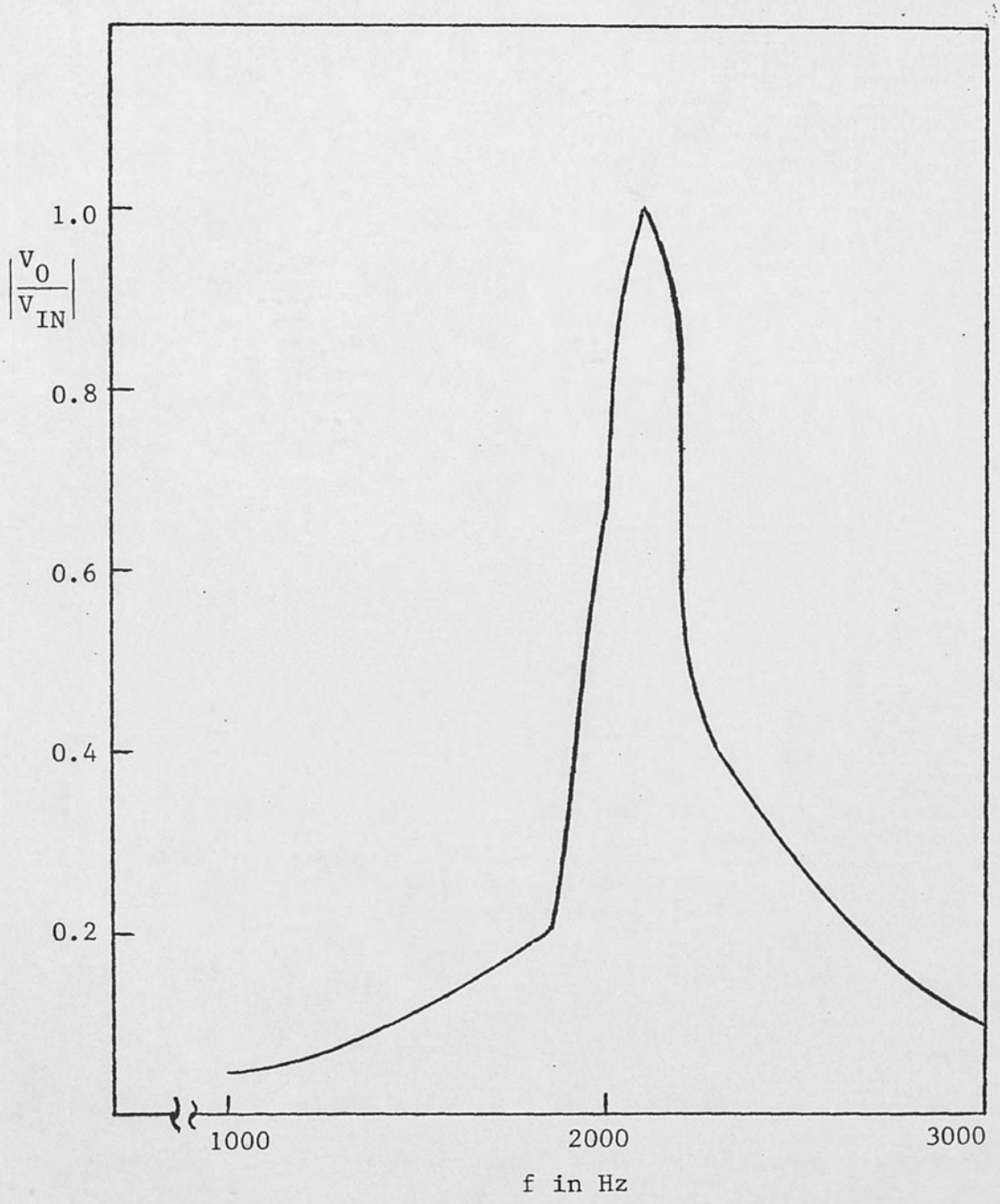

Fig. 2.9. Magnitude plot of Bandpass filter

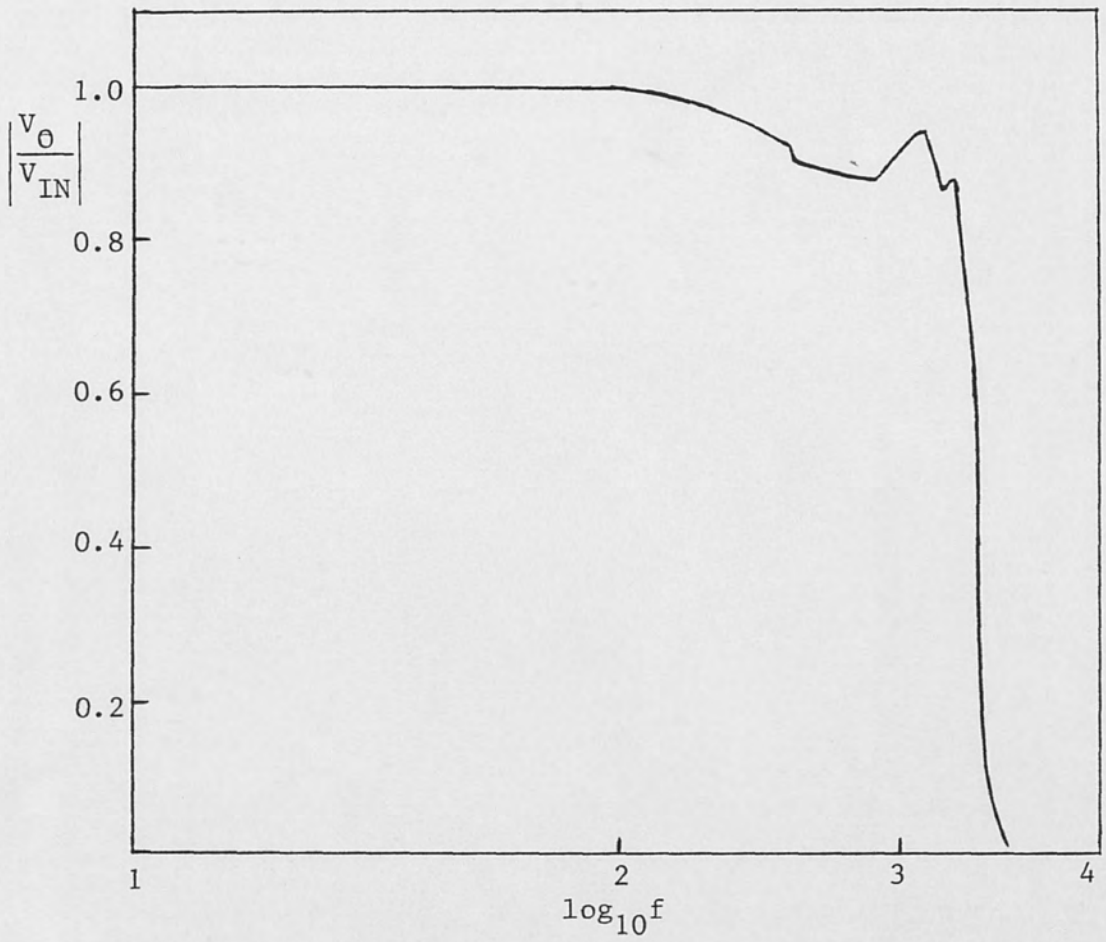

Fig. 2.10. Magnitude plot of Chebyshev lowpass filter

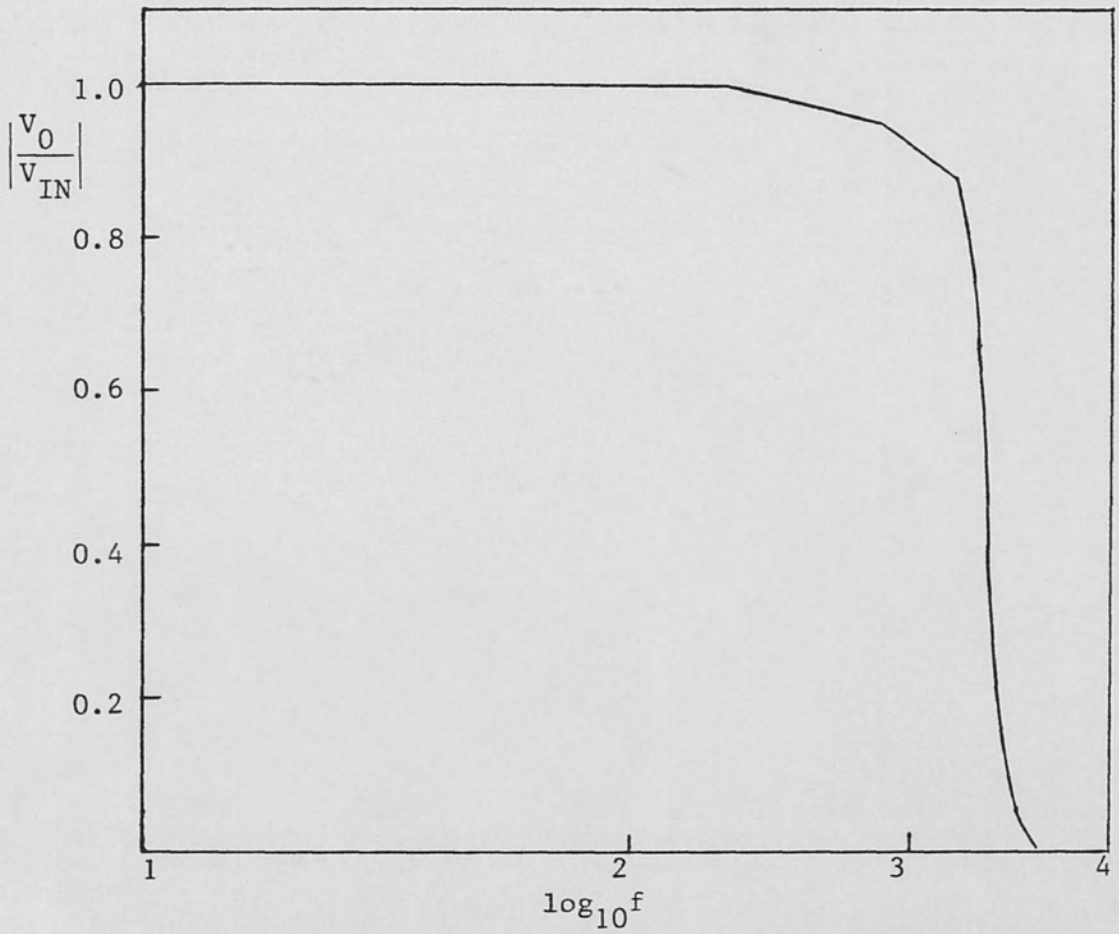

Fig. 2.11. Magnitude plot of Butterworth lowpass filter

APPENDIX 3

COMPUTER PROGRAMS

Computer program #1 represents a Fortran program used to transform lowpass pole positions into the equivalent bandpass pole positions. FN, Q and QBP are the program inputs. FN and Q are the lowpass filter parameters whose values can be obtained in Burr Brown 1979 General Catalog (Table 1 p. 4-104). QBP is the desired Q of the bandpass filter.

```
      COMPLEX P,S,U
      READ 5,FN,Q,QBP
    5 FORMAT ( 3F12.5 )
      Y=FN*SQRT(1.-(1./(Q*2.))**2)
      X=-FN/(Q*2.)
      P=CMPLX(X,Y)
      U=CONJG(P)
      DO 30 I=1,2
      S=P/(2.*QBP)
      P=S**2-1
      T=ATAN2(AIMAG(P),REAL(P))
      IF(T.GE.0.)GO TO 10
      T=2.*3.14159+T
   10 T=T/2.
      A=SQRT(CABS(P))*COS(T)
      B=SQRT(CABS(P))*SIN(T)
      S=S+CMPLX(A,B)
      FN=CABS(S)
      Q=-FN/(2.*REAL(S))
      PRINT 20,FN,Q
   20 FORMAT( 10X,'FN = ', F12.5,2X,'Q = ',F12.5)
      IF(AIMAG(U).EQ.0.) GO TO 40
   30 P=U
   40 STOP
      END
```

Computer program #2 is a Basic program that may be used to calculate the first and second moments at four different locations in a network. The program inputs are the number of data points (P) to be sampled and the sample rate in hertz (R).

```
10 DIM V%(4999)
20 PRINT 'ENTER THE NUMBER OF DATA POINTS ';
30 INPUT P
40 IF P>4999 GO TO 20
50 PRINT 'ENTER THE SAMPLE RATE IN HERTZ ';
60 INPUT R
70 R1=1/R
80 AIN('FAST',V%(),P,R1,0,1)
90 PRINT ' SAMPLING IS DONE.'
100 FOR X = 0 TO (P-1)
110 A=V%(X)*5.11743/2047
120 I1=A+I1
130 I2=A*A+I2
170 NEXT X
180 I1=I1/P
190 I2=I2/P
200 PRINT ' I1,I2 ARE THE FIRST,SECOND MOMENT AT THE OUTPUT OF
    LOWPASS FILTER'
270 PRINT 'I1    I2'
280 PRINT I1,I2
290 AIN('FAST',V%(),P,R1,1,1)
300 PRINT 'SAMPLING IS DONE'
310 FOR X=0 TO(P-1)
320 B=V%(X)*5.11743/2047
330 J1=B+J1
340 J2=B*B+J2
350 NEXT X
360 J1=J1/P
370 J2=J2/P
375 PRINT ' J1,J2 ARE THE FIRST,SECOND MOMENT OF NOISE FROM 1'
380 PRINT 'J1    J2'
390 PRINT J1,J2
400 AIN('FAST',V%(),P,R1,2,1)
410 PRINT 'SAMPLING IS DONE'
420 FOR X=0 TO (P-1)
430 C=V%(X)*5.11743/2074
440 K1=C+K1
450 K2=C*C+K2
460 NEXT X
470 K1=K1/P
480 K2=K2/P
```

```
485 PRINT ' K1,K2 ARE THE FIRST,SECOND MOMENT OF NOISE FROM 2'
490 PRINT 'K1    K2'
500 PRINT K1,K2
510 AIN('FAST',V%(),P,R1,3,1)
520 PRINT 'SAMPLING IS DONE'
530 FOR X=0 TO (P-1)
540 D=V%(X)*5.11743/2074
550 L1=D+L1
560 L2=D*D+L2
570 NEXT X
580 L1=L1/P
590 L2=L2/P
595 PRINT ' L1,L2ARE FIRST,SECOND MOMENT OF SIGNAL'
600 PRINT 'L1    L2'
610 PRINT L1,L2
620 PRINT ' S1 IS INPUT SIGNAL TO NOISE RATIO OF CHANNEL 1'
630 S1=(.98*L2)/J2
640 PRINT ' S2 IS INPUT SIGNAL TO NOISE RATIO OF CHANNEL 2'
650 S2=(.98*L2)/K2
660 PRINT 'S0 IS OUTPUT SIGNAL TO NOISE RATIO'
670 S0=I1*I1/(I2-I1*I1)
680 PRINT 'S1','S2','S0'
690 PRINT S1,S2,S0
700 END
```

LIST OF REFERENCES

Abramowitz, M., and Stegun, I., eds. Handbook of Mathematical Functions. New York: Dover Publishing Company, 1965.

Allgaier, D. E. "A Comparison of Output Signal to Noise Ratio of Cross-Correlators with Bandpass Inputs." Master of Science Research Report, University of Central Florida, 1979.

Andrews, L. C. "The Probability Density Function for the Output of a Cross Correlator with Bandpass Inputs." IEEE Transactions Information Theory IT-19 (January 1973): 13 - 19.

_____. "The Output pdf of a Polarity Coincidence Correlation Detector." IEEE Transactions Aerospace and Electronic Systems AES-10 (September 1974): 712 - 715.

_____. "Analysis of a Cross Correlator with a Clipper in One Channel." IEEE Transactions Information Theory IT-26 (November 1980): 743 - 746.

Brown, J. L., Jr., and Piper, H. S., Jr. "Output Characteristic Function for an Analog Cross-Correlator with Bandpass Inputs." IEEE Transactions Information Theory IT-13 (January 1967): 6 - 10.

Burr Brown. General Catalog. Tucson, AZ: Burr Brown, 1979.

Cheng, M. C. "Clipping Loss in Correlation Detectors for Arbitrary Input Signal-To-Noise Ratios." IEEE Transactions Information Theory IT-14 (May 1968): 338 - 389.

Cooper, D. C. "The Probability Density Function for the Output of a Cross-Correlator with Bandpass Inputs." IEEE Transactions Information Theory IT-11 (April 1965): 190 - 195.

Cooper, G. R., and McGillen, C. D. Probabilistic Methods of Signal and System Analysis. New York: Holt, Rinehart and Winston, 1971.

Daryanani, G. Principles of Active Network Synthesis and Design. New York: John Wiley & Sons, 1976.

Ekre, H. "Polarity Coincidence Correlation Detection of a Weak Noise Source." IEEE Transactions Information Theory IT-9 (January 1963): 18 - 23.

Faran, J. J., and Hills, R., Jr. "Correlators for Signal Reception." Cambridge, MA: Harvard University Acoustical Research Laboratory. (Technical Memorandum 27, 1952).

Green, P. E. "The Output Signal-To-Noise Ratio of Correlation Detectors." IRE Transactions Information Theory IT-3 (March 1957): 10 - 18.

Lange, F. H. Correlation Techniques. New Jersey: D. Van Nostrand, 1967.

Rice, S. O. "Mathematical Analysis of Random Noise." Bell Systems Technical Journal 23 (July 1944): 282 - 332; continuation Bell Systems Technical Journal 24 (January 1945): 46 - 156.

Roberge, J. K. Operational Amplifiers Theory and Practice. New York: John Wiley & Sons, 1975.